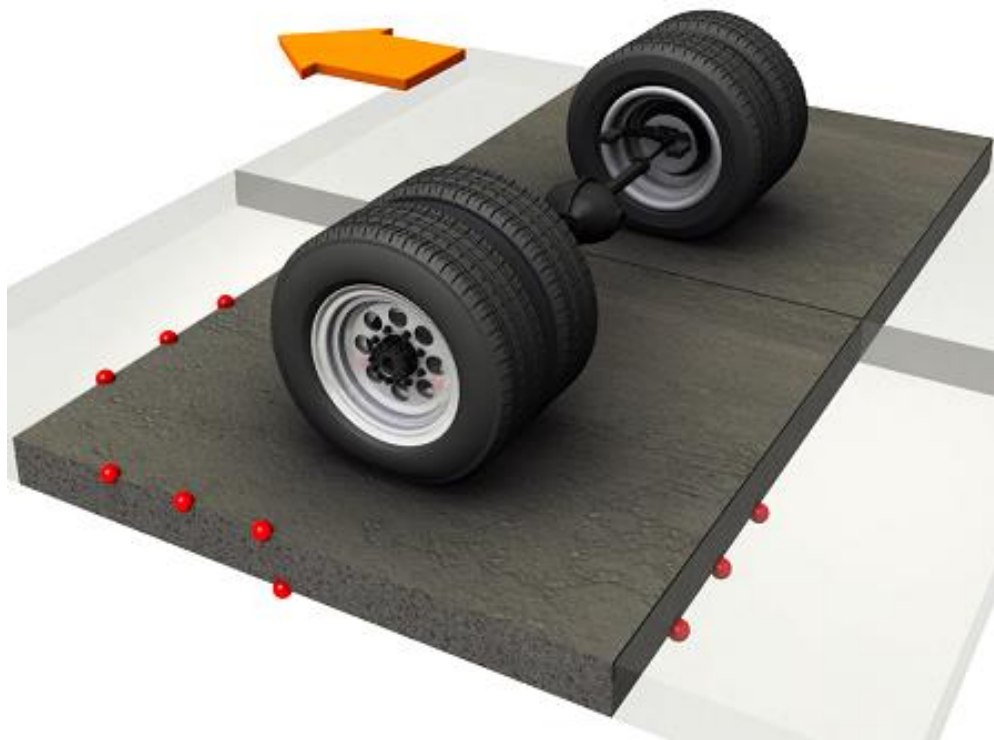


# Documentation and Design Guide

## OptiPave 2®



## Optipave2 v2.0

### Introduction

Typical slab dimensions for a concrete pavement are 3.6 m wide by 4.5 m long (AASHTO 1993), with slab thicknesses ranging from 15 to 35 cm, depending on the level of traffic, the climate, and the materials used. The required thickness is primarily dependent on the axle weight and number of load repetitions, concrete strength, slab length, and temperature differential. Besides temperature curling, construction curling can have a significant effect on the stress state in concrete slabs.

In order to reduce the interacting effects of loading and curling stresses, a new pavement design methodology has been proposed to design concrete slabs by optimizing the slab size given the geometry of the expected truck traffic (Covarrubias and Covarrubias 2008). In this design approach, slabs sizes are chosen such that no more than one set of wheels from a truck axle are on any given slab. By distributing the mechanical loads over multiple slabs, tensile stresses are reduced, as are the curling stresses, due to the reduced slab dimensions.

In order to validate this new design concept, several full-scale test sections were constructed and tested at the University of Illinois to understand the failure mode and fatigue life of this rigid pavement system (Cervantes and Roesler 2009). Furthermore, to generalize the design concept and results of the full-scale tests for a large variety of inputs, stress analyses had to be completed to account for cases that were not directly tested. The results from the stress analysis and full-scale investigation will be presented in this paper and combined into this design software.

The design method developed by TCPavements<sup>1</sup> is the result of years of studies and tests, based on fatigue damage equations of the project NCHRP 1-37<sup>o</sup> (NCHRP 2006) and with stress calculations computed with the finite element program ISLAB2000 (Khazanovich et al. 2000).

With the use of short slab sizes and the concomitantly reduced slab thickness, the pavement design method requires several other modifications in order to achieve the intended pavement service life. The following are a list of additional adjustments that must be made to the concrete pavement system to accommodate the optimized slab design.

---

<sup>1</sup> TCP technology (Thin Concrete Pavements), the methodology for the design and construction of improved concrete pavement slabs and other rights related to this technology (software, know-how, industrial secrets, trademarks, manuals, instructions, etc.), are exclusively owned by Comercial TCPavements Ltda. and subject to legal protection as recognized in local regulations and International Intellectual and Industrial Property Treaties, particularly by patent N°44820 in Chile, N° 7.571.581 US, N°5.940 Peru, international application PCT/EP2006/064732 among others. ©TCPavements 2005-2013, all rights reserved

1. Due to the larger number of contraction joints and the desire not to seal joints, thin saw blades with a 2 mm width should be used to limit spalling caused by incompressible material entering the joint.
2. Due to the quantity of unsealed contraction joints, it is necessary to have a granular base which is insensitive to moisture and minimizes pumping. The granular base material should have less than 8 percent material finer than the 75  $\mu\text{m}$  sieve, and a high CBR.
3. There should be a nonwoven geotextile layer between base and the natural soil to act as a separation layer. This geotextile prevents subgrade intrusion into the more freely draining base layer, and prevents aggregate penetration into the weaker subgrade soil.
4. Due to the large amount of saw cuts, load transfer is primarily carried by aggregate interlock and thus dowels and tie bars are not part of the standard design of this system. In order prevent the thinner slabs from moving laterally, the concrete slabs must also be restrained on the longitudinal edge with a concrete shoulder, vertical steel pins or incorporation of structural fibers.
5. For high volume designs, a targeted load transfer system should be used to ensure design life is achieved.

## 1. Optipave 2 Design Guide

### Introduction

Optipave 2 is a computer program developed by TC Pavements to design of jointed plain concrete pavements (JPCP) using a new design methodology which reduces the interacting effects of loading and curling stresses through optimized slab (Covarrubias and Covarrubias 2008). In this design approach, slabs sizes are chosen such that no more than one set of wheels from a truck axle are on any given slab. By distributing the mechanical loads over multiple slabs, tensile stresses are reduced, as are the curling stresses, due to the reduced slab dimensions. This software has been calibrated with the research conducted at the University of Illinois (Cervantes and Roesler 2009).

The inputs required by Optipave 2 can be divided into five categories, as given below. Each of these categories will be discussed in detail.

- Design ParametersTraffic
- Concrete Properties
- Support Layers
- Location/Climate

#### 1.1- Design Parameters

##### 1.1-1. Design Life

The design life is the expected service life of the pavement in years. Pavement performance is predicted over the design life beginning from the month the pavement is open to traffic. The design life can be selected depending of the road classification as shown in Table 1.

Table 1: Design life based on road classification

Road Classification	Design Life (Years)
Local routes and streets	15-20
Principal arterials < 15 <sup>6</sup> ESALS	20
National highways and high traffic routes > 15 <sup>6</sup> EE	20-40

##### 1.1-2. Joint Spacing

Joint spacing is the distance between two adjacent joints in the longitudinal direction, and is equal to the length of the slab. The selected joint spacing depends on the use of the pavement. If the pavement is in an area prone to high curling, the slabs must have a shorter joint spacing. The joint spacing varies between 5 and 7.5 ft. If the traffic path is in multiple directions, the joint spacing can be no longer than 5.5 ft to avoid two axles loading one slab diagonally.

**1.1-3. Concrete Slab Thickness**

Thickness of the concrete slab, which is one of the most critical parameters in obtaining the required performance, can vary between 2.5 and 9.5 inches. This design program allows the user to evaluate a trial design or calculate the optimum thickness by selecting the iterate thickness check box.

**1.1-4. Type of Edge**

The type of edge has two effects. First, it provides lateral support to the structure, and second, it increases the traffic wander distance from the edge. The software automatically changes these parameters, depending on the type of edge as shown in Table 2.

Table 2: Program parameters based on edge type

Type of edge	Structural support	Increases the traffic wander distance from the edge?
Free Edge	Null	No
Granular/Asphalt Shoulder	Very Slight	No
Tied Pcc Shoulder	Slight	No
Curb	Medium	Yes

**1.1-5. Widened Slabs**

The JPCP slab can be widened to accommodate the outer wheel path further away from the longitudinal edge. Widened slab can significantly improve JPCP performance because they result in reduced edge stresses and corner deflections. The structural effects of widened slabs are directly considered in the design process.

**1.1-6. Dowels on Transverse Joint**

Placement of dowels on transverse joints improves the load transfer efficiency and also reduces joint faulting on the transverse joint. Dowels are recommended on projects with high traffic (over 15,000,000 ESALs)

**1.1-7. Bond Type**

It is possible to add the option of calculating distresses of a concrete pavement bonded to an asphalt or concrete base.

**1.1-8. Initial IRI**

Initial IRI is the IRI when the pavement is opened to traffic.

**1.1-9. Percentage of Cracked Slabs**

The percentage of cracked slabs is the maximum admitted level of damage, given a certain level of reliability, at the end of the design life. This value depends of the importance of the road. Table 3 shows recommended values depending on the road classification.

Table 3: Recommended value for the percentage of cracked slabs based on road classification

Road Classification	Percentage of Cracked Slabs
Local routes and streets	30%-50%
Principal Arterials < 15^6 EE	10%-30%
National Highways and high traffic routes > 15^6 EE	10%

### 1.1-10. Terminal IRI

The terminal IRI is the maximum allowable IRI. If the IRI of the project exceeds this value, the pavement shall be subjected to any treatment that reduces this index. In general the maximum allowed IRI is 172 in/mile.

### 1.1-11. Terminal Mean Joint Faulting

The terminal mean joint faulting is the maximum allowable mean joint faulting. If the joint faulting exceeds this value, the pavement shall be subjected to any treatment that reduces this distress. In general the maximum allowed mean joint faulting is 0.12 in.

### 1.1-12. Reliability

Practically everything associated with the design of new and rehabilitated pavements is variable or uncertain in nature. Therefore, pavements exhibit significant variation in condition along their length. Even though mechanistic concepts provide a more accurate and realistic method for pavement design, a practical method to consider the uncertainties and variations in design is needed so that a new or rehabilitated pavement can be designed for a desired level of reliability. An analytical solution that allows the designer to design for a desired level of reliability for each distress and smoothness is available. Design reliability is defined as the probability that each of the key distress types and smoothness will be less than a selected critical level over the design period. Typical values of reliability for different road types are shown in Table 4.

Table 4: Reliability by road type

Functional Classification	Urban	Rural
Interstate/Freeways	85%-97%	80%-95%
Principal Arterials	80%-95%	75%-90%
Collectors	75%-85%	70%-80%
Local	50%-75%	50%-75%

## 1.2- Traffic

This design program has the feature of allowing the user to input traffic in two different ways:

- Traffic by Equivalent Axles
- Traffic by Load Spectra

### 1.2-1. Traffic by Equivalent Axles

The equivalent axle factor is a numerical factor that expresses the relationship of a given axle load to another axle load in terms of the relative effects of the two loads on the serviceability of a pavement structure. Typical equivalent axle factors for different road types are given in Table 5.

Table 5: Typical equivalent axle factors for different road types

Road Type	Equivalent Axle Factor
Local	EE 250.000
Collectors	EE 1.000.000
Principal Arterials	EE 10.000.000
Interstate/Freeways	EE 20.000.000

### 1.2-2. Traffic by Load Spectra

The following inputs are required for traffic by load spectra:

- Initial Two-Way AADTT ( $T_{MA_i}$ ): Average annual number of trucks and buses that travel on both directions on all lanes in one day.
- Percentage of Traffic in Design Direction ( $T_{DD}$ ): Percentage of heavy vehicles that travel on the design direction. The default value is typically 50%, but it may vary between 40% and 60%.
- Percentage of Traffic in Design Lane ( $T_{PD}$ ): Percentage of heavy vehicles that travel on the design direction. The default value is 90%, and varies between 50% (multiple lanes per direction) and 100% (one lane per direction).
- Percentage of Traffic in Summer: Percentage of heavy vehicles that travel on the design direction on the six hotter months of the season. This value is typically 50%.
- Total Traffic ( $T_{TOT}$ ): Total number of trucks that drive along the design lane, during the pavement design life. It can be obtained using the following formula:

$$T_{TOT} := T_{MA_i} \cdot \sum_{i=1}^{Vd} (1 + tc)^{i-1} \cdot T_{DD} \cdot T_{PD}$$

$$T_{TOT} := T_{MA_i} \cdot T_{DD} \cdot T_{PD} \cdot \sum_{i=1}^{Vd} (1 + tc)^{i-1}$$

$$T_{TOT} := T_{MA_i} \cdot T_{DD} \cdot T_{PD} \cdot \frac{((1 + tc)^{Vd} - 1)}{tc}$$

Where:

VD: Design Life of the Project.

**1.2-3. Annual Truck Traffic Growth**

The annual truck traffic growth factor is the mean growth percentage from one year to the next, based on the increase in traffic from the opening stage to the end of the design life. In general this value is 5%, and varies between 0% (no growth) and 10%.

**1.2-4. Type of Traffic**

The Federal Highway Administration classifies the traffic as a function of the types of vehicle that travel, from 1 to 17. The criteria for choosing the proper group are shown in Table 6 and Table 7.

Table 6: Applicable TTC Groups by Road Type

Functional Classification	Applicable TTC Group
Principal arterials, interstate & defense routes	1,2,3,4,5,8,11,13
Principal arterials, intrastate routes including freeways & expressways	1,2,3,4,6,7,8,9,10,11,12,14,16
Minor arterials	4,6,8,9,10,11,12,15,16,17
Major collectors	6,9,12,14,15,17
Minor collectors	9,12,14,17
Local routes & streets	9,12,14,18

Table 7: TTC Groups by Vehicle Type

Buses in Traffic Stream	Type Of Vehicle		Group TTC
	Percentage of Multi-Trailer Trucks	Percentage of Single-Trailers and Single Units Trucks	
Low to None (<2%)	Relatively High (>10%)	Predominantly single-trailer trucks	5
		High percentage of single-trailer trucks, but some single-unit trucks	8
		Mixed truck traffic with a higher percentage of single-trailer trucks	11
		Mixed truck traffic with about equal percentages of single-unit and single-trailer trucks	13
		Predominantly single-unit trucks	16
	Moderate (2 to 10%)	Predominantly single-trailer trucks	3
		Mixed truck traffic with a higher percentage of single-trailer trucks	7
		Mixed truck traffic with about equal percentages of single-unit and single-trailer trucks	10
		Predominantly single-unit trucks	15
		Low to Moderate (between 2 and 25%)	Low to None (<2%)
Predominantly single-trailer trucks, but with a low percentage of single-unit trucks	2		
Predominantly single-trailer trucks, but with a low to moderate amount of single-unit trucks	4		
Mixed truck traffic with a higher percentage of single-trailer trucks	6		
Mixed truck traffic with about equal percentages of single-unit and single-trailer trucks	9		
Mixed truck traffic with a higher percentage of single-unit trucks	12		
Predominantly single-unit trucks	14		
Major bus route (>25%)	Low to none (<2%)	Mixed truck traffic with about equal percentages of single-unit and single-trailer trucks	17

### 1.2-5. Truck Wander

One input of this design program is the distance between the outer edge of the wheel and the pavement marking, and the traffic wander standard deviation. The default values are  $\mu = 18$  in. and standard deviation = 10 in, see Figure 1.

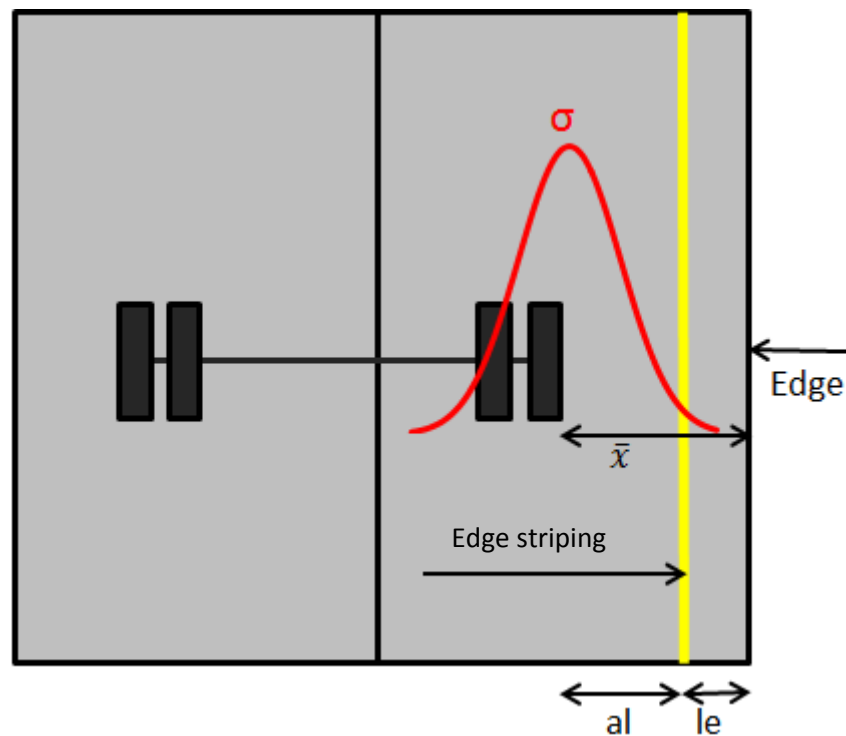


Figure 1: Typical traffic wander distribution

### 1.2-6. Effects of Curbs and Widened Slabs on Traffic Wander

When using widened slabs or curb on the edge, the distance between the outer wheel tire edge and the edge of the slab increases significantly compared with the other three types of edge. Curbs increase the distance between the edge striping and the other wheel tire edge ( $a_l + l_c$ ), and decrease the standard deviation of the traffic wander, as shown in Figure 2.

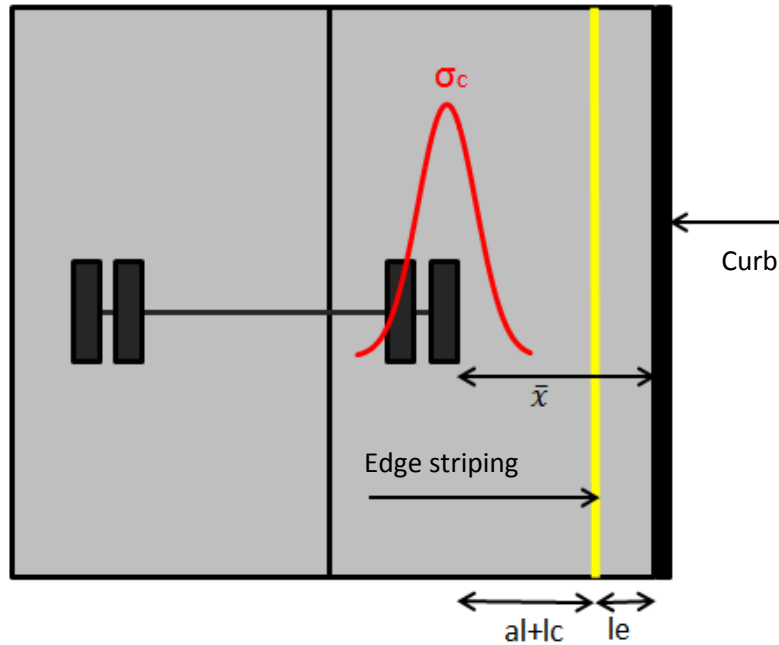


Figure 2: Effects of a curb on traffic wander

The effect of widened slabs is similar to the effect of curbs on the pavement shoulder, as it increases the distance of the wheels from the edge of the pavement slabs. However, in this case the increase is because of an increase in the distance between the edge striping and the edge of the pavement slabs, see Figure 3.

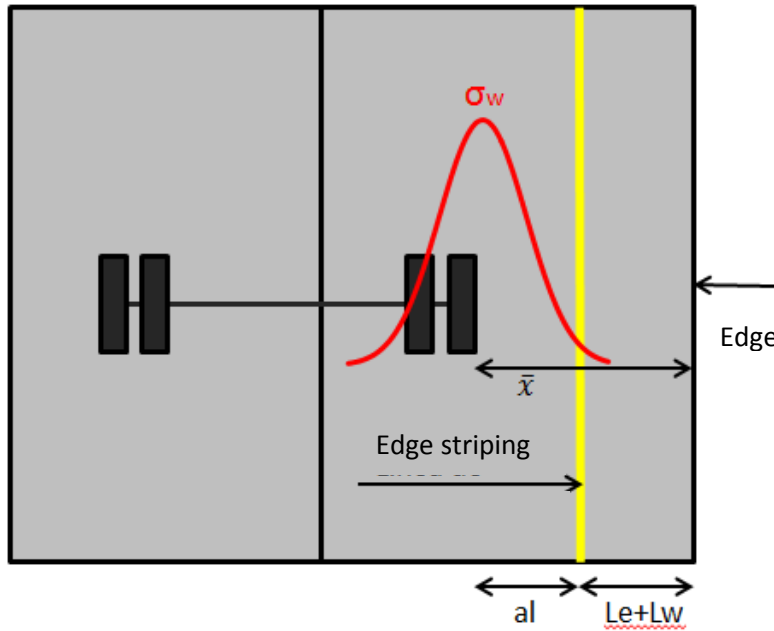


Figure 3: Effects of a widened lane on traffic wander

Default values of the distance between the edge and the outer edge of the axle tire for different edge types are shown in Table 8.

Table 8: Distance between the edge and the tire for different edge types

Type of Edge	Distance Between the edge and the lane marking	Distance between the lane marking and the outer edge of the tire	Distance between the edge and the outer edge of the axle tire
Free Edge, Tied Pcc Shoulder, Granular/Asphalt Base,	6 inches	18 inches	24 inches
Curb	6 inches	22 inches (18+4 inches)	28 inches
Widened Slabs	12 inches (6+6 inches)	18 inches	30 inches

Default values of mean traffic wander standard deviation for different types of edges are shown in Table 9.

Table 9: Standard deviation of mean traffic wader for different edge types.

Type of Edge	Mean traffic wander standard deviation
--------------	--

Free Edge, Tied Pcc Shoulder, Granular/Asphalt	10 inches
Curb	8 inches (10-2 inches)
Widened Slabs	10 inches (10+0 inches)

### 1.3- Concrete Properties

#### 1.3-1. Concrete Strength

Concrete strength in pavement is usually measured with a flexural strength test. This design program allows the user to determine the strength of the concrete by cubic and cylindrical compressive tests, and flexural-compressive strength relationships with factors which can be calibrated. Typical values of 28 day flexural strength for different road types are shown in Table 10.

Table 10: Concrete 28 day flexural strength based on road classification

Road Classification	28 Days Flexural Strength [PSI]
Collectors/Local Roads	650-725
Principal Arterials <math>15 \times 10^6</math> EE	700-750
Interstate/freeways >math>15 \times 10^6</math> EE	725-800

#### 1.3-2. Reliability of the Design of the Concrete

Usually a value of 80% is specified for the level of reliability of the concrete mixture.

#### 1.3-3. Standard Deviation

Generally, a value of 58 PSI is used for the standard deviation during the production of the concrete, see Figure 4

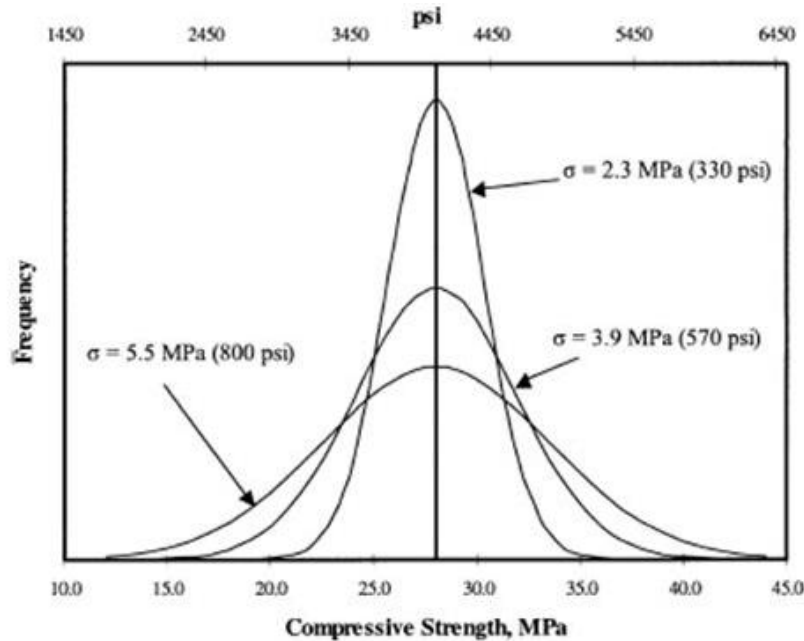


Figure 4: Effect of the standard deviation during concrete production

#### 1.3-4. 28-90 Days Strength Gain

The percentage of strength gained between day 28 and day 90 of the concrete may vary among each mixture, but a default value of 1.1 is generally used (10% gain).

#### 1.3-5. Modulus of Elasticity of Concrete

The modulus of elasticity of the concrete can be determined by direct testing or by using a relationship with compressive strength. A value of 4,200,000 psi is assumed for the modulus of elasticity. It can also be estimated by the following relationship:

$$E_c = 57.600 \cdot \sqrt{f'_c}$$

Where:

$E_c$ : Modulus of Elasticity [psi]

$f'_c$ : Cylinder Compressive Strength [psi]

#### 1.3-6. Residual Strength of Concrete

One feature of Optipave is the possibility to evaluate the performance of fiber reinforced concrete pavements. The effect of fibers is taken into account by the residual strength. The residual strength is the strength provided by the fiber after the concrete has cracked. This strength can be determined through three different methods:

- ASTM 1609-10

- Doble Punching (UNE 83515-2010)
- ASTM C1399-10

### 1.3-7. Unit Weight of Concrete

The default value of the self-weight of the concrete in a certain volume is 150 pcf.

### 1.3-8. Poisson's Ratio

Poisson's ratio is the ratio of transverse to axial strain, due to a load in the axial direction. The effect of this parameter is low, therefore is rarely measured through testing. The Poisson's ratio of concrete is often assumed to be 0.15 and ranges from 0.1 to 0.25

### 1.3-9. Coefficient of Thermal Expansion

The coefficient of thermal expansion is defined as the change in unit length per degree of temperature change. The magnitude of curling stresses is very sensitive to the coefficient of thermal expansion, thus it plays a key role in predicting JPCP performance. The value of the coefficient of thermal expansion is a function of the type of aggregate of the concrete, as shown in Table 11.

Table 11: Coefficient of thermal expansion of concrete based on aggregate type

Type of Aggregate	Coefficient of Thermal Expansion ( $10^{-6}/^{\circ}\text{F}$ )
Granite	4-5
Basalt	3.3-4.4
Limestone	3.3
Dolomite	4-5.5
Sandstone	6.1-6.7
Quartzite	6.1-7.2
Marble	2.2-4

### 1.3-10. Concrete Shrinkage at 365 Days

Shrinkage in concrete is a very important input which greatly affects the load transfer efficiency of a transverse joint. As shown in Figure 5, concrete will shrink as long as it is drying (low ambient relative humidity). When exposed to rewetting (high ambient relative humidity), it will swell, though it will not necessarily return to its original, pre-dried size because a portion of the shrinkage is irreversible. It should be noted that Figure 5 is highly idealized and the values presented in the figure are not necessarily applicable to Chilean concrete pavements. The default value of shrinkage strain used in this software is 0.0007 (700 $\mu\epsilon$ ).

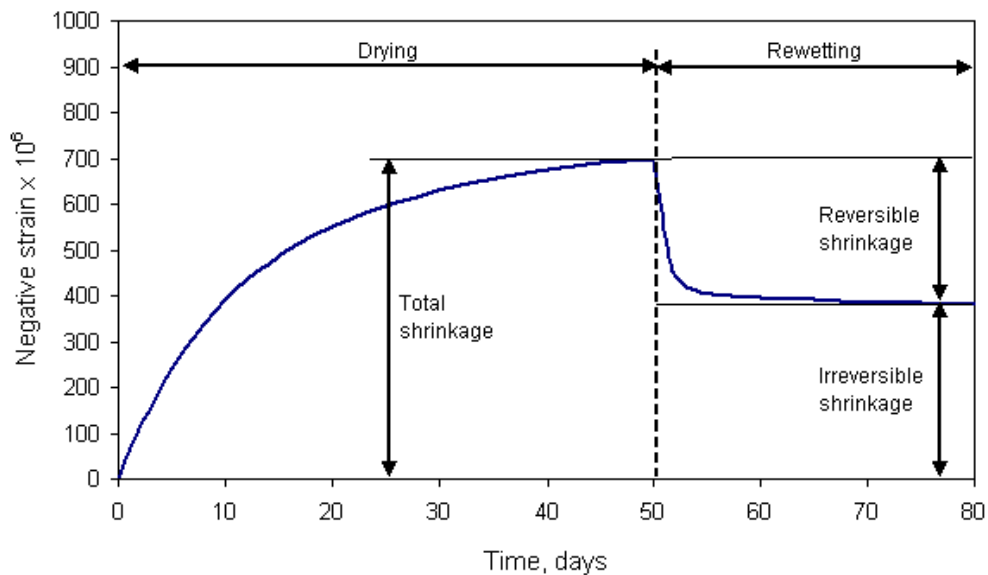


Figure 5: Shrinkage behavior of concrete during drying and rewetting.

#### 1.3-11. Air Content

Percentage of air contained on the concrete mixture

#### 1.3-12. Water/Cement Ratio

Amount of water per unit of cement on the mixture

### 1.4- Support Layers

#### 1.4-1. Number of Supporting Layers

Add the number of soil layers, without considering the subgrade as a layer. Up to six layers can be entered.

#### 1.4-2. Specify type of Soil Test

There are three possible types of test in this design program to determine the resilient modulus of the subgrade. These are:

- LAB: Measurements with a triaxial test.
- CBR: Measurements through correlations with the CBR test.
- FWD: Measurement with a Falling Weight Deflectometer.

#### 1.4-3. Resilient Modulus of each Layer

The resilient modulus of each layer must be entered. For the subgrade, the modulus during winter-time must be entered and the program calculates a different value during summer-time.

#### **1.4-4. Poisson's Ratio**

The Poisson's ratio of each layer must be entered. Values of typical values of these input can be seen pressing the help button.

#### **1.4-5. Layer Thickness**

The thickness of each layer must be entered.

#### **1.4-6. Base Erodibility**

The potential for the layer directly beneath the PCC layer to erode has a significant impact on the initiation and propagation of pavement distress. Different base types are classified based on long-term erodibility behavior as follows:

- Class 1- Extremely erosion resistant materials
- Class 2- Very erosion resistant materials
- Class 3- Erosion resistant materials
- Class 4- Fairly erodible materials
- Class 5- Very erodible materials

#### **1.4-7. Pavement-Soil Friction Coefficient**

Friction coefficient between the base and the pavement, which directly affects the load transfer efficiency of the system. It is typical to use a value of 0.65 on granular base and 0.8 on a cement treated base.

#### **1.4-8. Percentage of fine material on the subgrade**

Percentage of the subgrade material that passes the N°200 sieve.

#### **1.4-9. Support Layer Processing**

After all the different inputs for the support layers are entered, the soil model calculates the combined k-value, using the K-SEM method. Because there can be a major difference between summer-time and winter-time soil properties, the soil models calculate different values for each season.

#### **1.4-10. K-SEM Method**

The required data are the material characteristics (Modulus of elasticity, Poisson's ratio) and the thickness of each layer. The radius of the circular load plate is constant. It is important to consider the proper material properties of each layer (i.e. the Poisson's ratio and modulus of elasticity), which are used to calculate a static modulus of subgrade reaction. However, it is common to work with the resilient modulus of the materials, which result in a relatively larger value of static modulus. Therefore, the software incorporates the option of using modulus of elasticity or resilient modulus. When using the

resilient modulus, the calculated modulus of subgrade reaction is multiplied by 0.5. A schematic of a typical multilayer system which can be used with the K-SEM method is shown in Figure 6

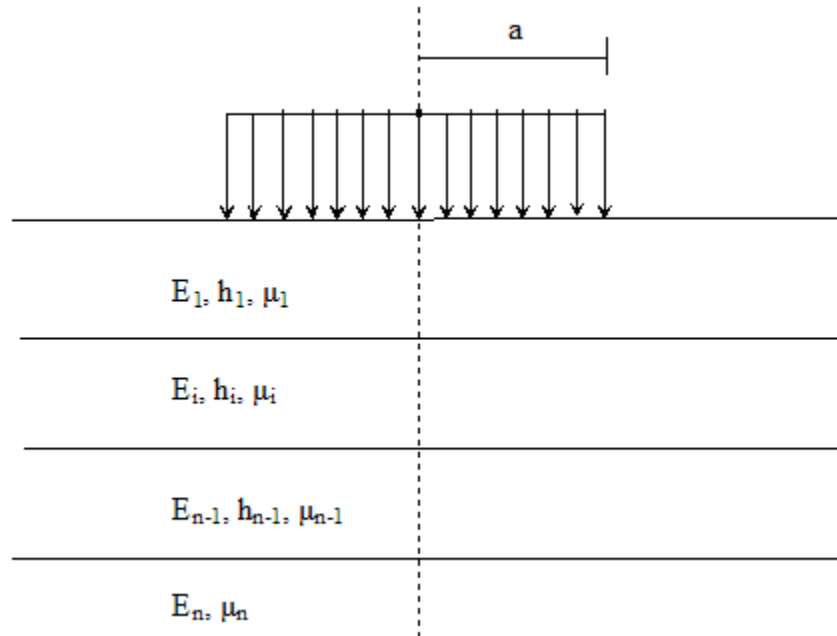


Figure 6: Scheme of a multi-layer system

Where:

$E_i$  = Modulus of elasticity of layer  $i$

$h_i$  = Thickness of layer  $i$

$\mu_i$  = Poisson's Ratio of layer  $i$

$a$  = Radius of load plate (15 in)

#### Equivalent Reaction Modulus

The calculated equivalent modulus of reaction comes from the deflection of the surface generated by a rigid load plate. This method simulates the rigid plate test quickly and accurately. The formulas required for this method are given below.

For a semi-infinite layer (one layer)

$$k = \frac{1.273 \cdot E}{2(1 - \mu^2)a}$$

For two or more layers:

$$k = \frac{0.0167087 \cdot E_n}{(1 - \mu^2) \left[ \frac{\left(1 - \frac{E_n}{\hat{E}}\right)}{\left[1 + \left(\frac{h_1 + h_2 + \dots + h_{n-1}}{38.1}\right)^2 \left(\frac{\hat{E}}{E_n}\right)^{2/3}\right]^{3/2}} + \frac{E_n}{\hat{E}} \right]}$$

Where:

$$\hat{E} = E_1 \left[ \frac{h_1 + h_2 \sqrt[3]{\frac{E_2}{E_1}} + h_3 \sqrt[3]{\frac{E_3}{E_1}} + \dots + h_{n-1} \sqrt[3]{\frac{E_{n-1}}{E_1}}}{\sum_{i=1}^{n-1} h_i} \right]^3$$

$\hat{E}$  = Equivalent Modulus

$E_i$  = Modulus of elasticity of layer i

$h_i$  = Thickness of layer i

$\mu_n$  = Poisson's Ratio layer n

### 1.5- Location/ Climate

Climate data is included in the Optipave 2 software. The software calculates many temperature differentials between the top and bottom surfaces of the slab, and depending on the location of the project, a certain temperature differential distribution. The software includes four generic climates:

- Wet- Freeze
- Wet-Non Freeze
- Dry- Freeze
- Dry-Non Freeze

#### 1.5-1. Built-in Curling

The built-in curling is an estimation of the initial curling which is a consequence of the differential shrinkage between the top and bottom part of the slab and the presence of a temperature gradient during the time of set of the concrete. This gradient is expressed as a thermal gradient (°F) which would be needed to flatten the slab. This value depends on the year season where is built, and the climate of the location of the project. There is not enough information currently known about this value, but the following list can be used as a guide:

- Wet Zone without Wind -10°F.
- Wet Zone with Wind and Dry Zone without Wind -20°F
- Dry Zone with Wind and Zone with high altitude -30° F
- Extreme Conditions of Water Evaporation -40°F

**1.5-2. Mean Winter Temperature**

The mean winter temperature is the mean temperature during the six colder months of the year.

**1.5-3. Mean Summer Temperature**

The mean summer temperature is the mean temperature during the six hotter months of the year.

**1.5-4. Concrete Setting Temperature**

The concrete setting temperature is the maximum temperature of the concrete during the hardening process, which occurs on the first 24 hours.

**1.5-5. Mean Annual Rainfall**

The mean annual rainfall is the average value of rainfall during one year on the location of the project.

**1.5-6. Base Freezing Index**

Percentage of time in the year, that the base is below 32°F.

## 2. Optipave 2

The latest design programs, such as the M-E PDG, incorporate stress prediction based on finite elements runs and neural networks on the structural analysis of pavements. Therefore, TCP developed a new software, called Optipave 2, which incorporates these features.

### 2.1- Types of Distresses on Concrete Pavements

The Optipave 2 design program evaluates five types of distresses:

- Bottom-up Transverse Cracking
- Bottom-Up Longitudinal Cracking
- Top-Down Corner Cracking
- Joint Faulting
- Smoothness (IRI)

#### 2.1-1. Bottom-Up Transversal Cracking

This type of distress is a crack that originates at the bottom edge of the slab and propagates transversely until reaching the top of the slab, due to the fatigue of the concrete. This type of cracking may occur when the traffic wheel path is near the pavement edge-shoulder joint.

#### 2.1-2. Bottom-Up Longitudinal Cracking

This type of distress is a crack that originates at the bottom of the transversal joint, at a variable distance from the edge and propagates upward and longitudinally until reaching the top of the slab, due to fatigue on the concrete.

#### 2.1-3. Top-Down Corner Cracking

Corner cracking may occur on the top of the transverse joint or on the top of the slab shoulder, depending on load transfer efficiency and traffic wheel path. In the first case, it propagates diagonally, descending until reaching the transverse joint and the bottom face of the slab. In the second case, it propagates diagonally in the other direction, until reaching the pavement edge/shoulder joint and the lower face of the slab.

#### 2.1-4. Mean Joint Faulting

Joint faulting is an important issue in the serviceability of a pavement. Joint faulting is the result of a difference in the level of one slab relative to the adjacent slab.

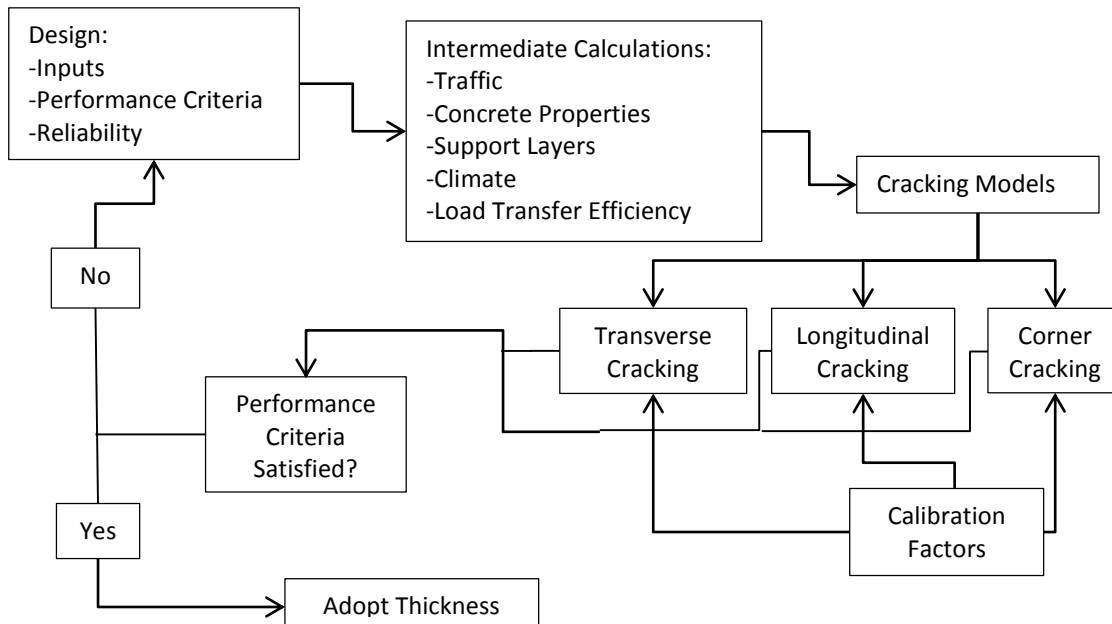


Figure 7 Flow chart of the TCP design process

## 2.2- Equivalent Structure Concept

There are an infinite number of possible combinations of design variables, such as traffic, properties of concrete, properties of support layers and climatic properties. The solution for this issue is the equivalent structure concept (Khazanovich 1994; Khazanovich et al. 2001), as illustrated in Figure 8, and neural network training. The use of this method is explained below.

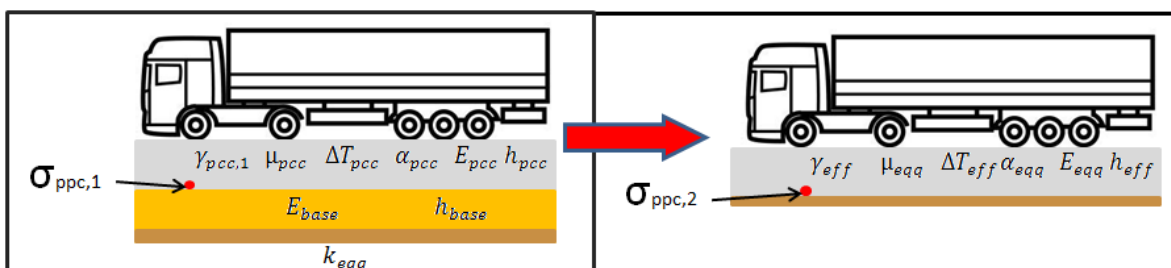


Figure 8: Illustration of turning a two layer system (left) into an equivalent single layer system (right).

### 2.2-1. Compute $h_{eff}$ for Unbonded or Bonded Pavements:

For the unbonded case, the effective thickness of an equivalent single layer system is (Ioannides et al. 1992):

$$h_{eff} := \sqrt[3]{h_{PCC}^3 + \frac{E_{base}}{E_{PCC}} \cdot h_{BASE}^3 + \dots}$$

Where:

$h_{eff}$ : Effective Thickness

$h_{PCC}$ : Concrete layer Thickness

$E_{BASE}$ : Resilient Modulus of the Base

$E_{PCC}$ : Elastic Modulus of Concrete

$h_{BASE}$ : Base Thickness

For the bonded case, the effective thickness for an equivalent single layer system is (Ioannides et al. 1992):

$$h_{eff} := \sqrt[3]{h_{PCC}^3 + \frac{E_{base}}{E_{PCC}} \cdot h_{Base}^3 + 12 \left( h_{PCC} \left( x - \frac{h_{PCC}}{2} \right)^2 + \frac{E_{Base}}{E_{PCC}} \left( h_{PCC} + \frac{h_{Base}}{2} - x \right)^2 h_{Base} \right)}$$

Where:  $x$  = Distance between the neutral axis and the top surface of the concrete layer, which can be calculated using the next formula:

$$x := \frac{\frac{h_{PCC}^2}{2} + \frac{E_{Base}}{E_{PCC}} h_{Base} \left( h_{PCC} + \frac{h_{Base}}{2} \right)}{h_{PCC} + \frac{E_{Base}}{E_{PCC}} h_{Base}}$$

### 2.2-2. Calculate the Effective Temperature Differential:

For the unbonded case (Ioannides and Khazanovich 1998):

$$\Delta T_{eff} := \frac{h_{PCC}^2}{h_{eff}^2} \cdot \Delta T$$

For the bonded case (Ioannides and Khazanovich 1998):

$$\Delta T_{eff} := \frac{h_{PCC} \cdot \Delta T \cdot (6 \cdot x - 2 \cdot h_{PCC})}{h_{eff}^2}$$

### 2.2-3. Calculate Effective Unit Weight ( $\gamma_{eff}$ )

For the unbonded case (Khazanovich 1994):

$$\gamma_{eff} := \frac{\gamma_{PCC} \cdot h_{PCC}}{h_{eff}}$$

Where:

$\gamma_{eff}$ : Effective Unit Weight

$\gamma_{PCC}$ : Concrete Unit Weight

$h_{eff}$ : Effective Thickness

$h_{PCC}$ : Effective Concrete Layer

#### 2.2-4. Compute the Radius of Relative Stiffness ( $l$ )

For both the bonded and unbonded cases (Westergaard 1927):

$$l = \sqrt[4]{\frac{E_{PCC} h_{eff}^3}{12 * (1 - \mu^3) * k}}$$

$l$ : Radius of relative Stiffness

$E_{PCC}$ : Modulus of Elasticity of Concrete

$h_{eff}$ : Effective Thickness

$\mu$ : Poisson's Ratio

$k$ : Modulus of subgrade Reaction

#### 2.2-5. Korenev's Non-dimensional Temperature Gradient

For both the bonded and unbonded cases (Korenev and Chernigovskaya 1962):

$$\phi = \frac{2\alpha_{PCC}(1 + \mu_{PCC})l^2 k}{h_{eff}^2 \gamma_{eff}} \Delta T_{eff}$$

$\phi$ : Korenev Non-dimensional Temperature Gradient

$\alpha_{PCC}$ : Coefficient of Thermal Expansion

$\mu_{PCC}$ : Poisson's Ratio of Concrete

$l$ : Radius of Relative Stiffness

$k$ : Modulus of subgrade Reaction

$h_{eff}$ : Effective Thickness

$\gamma_{eff}$ : Effective Unit Weight

$\Delta T_{eff}$ : the Effective Temperature Differential

#### 2.2-6. Equivalent Structure Concept

From the equivalent structure concept (Khazanovich et al. 2001), if the following conditions are fulfilled, then the stresses of one structure are equivalent than the other:

$$l_1 = l_2$$

$$L_1 = L_2$$

$$\Phi_1 = \Phi_2$$

$$\frac{AGG_1}{k_1 l_1} = \frac{AGG_2}{k_2 l_2}$$

$$\frac{P_{a,1}}{h_{pcc,1} \gamma_{pcc,1}} = \frac{P_{a,2}}{h_{pcc,2} \gamma_{pcc,2}}$$

$$s_1 = s_2$$

Where:

$l$ : Radius of Relative Stiffness

$L$ : Slab Length (Joint Spacing)

$\Phi$ : Radius of relative Stiffness

AGG: Aggregate Joint Stiffness

$P_a$ : Axle Load

$\gamma_{pcc}$ : Concrete unit weight

$s$ : Distance between the pavement shoulder and the outer wheel tire edge

1 and 2: Slabs 1 and 2 respectively

### 2.2-7. Footprint Correction

The equivalent structure concept requires the stress be corrected due to the influence of the size of the tire footprint. In the ISLAB-2000 runs, only a tire pressure of 8.2 kg/cm<sup>2</sup> was used. For small width tires, the load is higher than the actual load, and the footprint is bigger than in reality. Therefore an extra stress must be added, because larger footprints produce lower stresses. For tire widths larger than 15 cm, the effect is the opposite and must also be corrected for.

If the conditions outlined in section 2.2-6 are satisfied, and the footprint correction stresses  $\sigma_{NN,FP}$  are appropriately computed, then the stress of any slab (1) is a function of the stress computed on the neural network (2) as follows:

$$\sigma_{pcc,1} = \frac{h_1^2 h_2 \gamma_1}{h_{eff}^3 \gamma_2} (\sigma_{pcc,2} - \sigma_{NN,FP}) - \frac{E_{pcc,1}}{1 - \mu_{pcc,1}} \alpha_{pcc,1} \cdot \left( \frac{h_{eff}^3 - h_{pcc}^3}{2 \cdot h_{eff}^3} \right) \cdot (T_{top} - T_{bot})$$

Where:

$\sigma_{NN,FP}$ : Footprint Correction Stress

$$\sigma_{pcc,2} = \sigma_{NN} \left( l_1, L_1, \varphi_1, \frac{AGG_1 k_2 l_2}{k_1 l_1}, \frac{P_{a,1} h_{pcc,2} \gamma_{pcc,2}}{h_{pcc,1} \gamma_{pcc,1}} \right)$$

### 2.3- Tensile Stresses by a Finite Element Program (Islab2000):

Using ISLAB 2000 finite element software (Khazanovich et al. 2000), several runs were conducted to obtain the stresses for longitudinal, transverse and corner cracking, and also the deflections for the faulting model. Due to the fact that ISLAB 2000 is a dimensional program, the metric system was used. The following design inputs were considered:

#### 2.3-1. Design Inputs

##### 2.3-1.1. Slab Joint Spacing

Three Joint different spacing were considered:

- 1.4 m
- 1.8 m
- 2.3 m

Two different slab widths were considered:

- 1.8 m
- 2.1 m (widened slabs).

##### 2.3-1.2. Axle Types and Loads:

Two different axle types were considered: Single Axle and Tandem Axle. For the single axles, the axel loads were: 0, 3000, 6000, 12000, 16000, 25600 and 40000 Kg. For the tandem axles, the axle loads were: 0, 6000, 12000, 24000, 32000, 50000 and 80000 Kg.

##### 2.3-1.3. Axle Configuration

The axel configurations are shown in Table 12 for the single axle case and Table 13 for the tandem axle case.

Table 12: Axle configuration for the single axle case

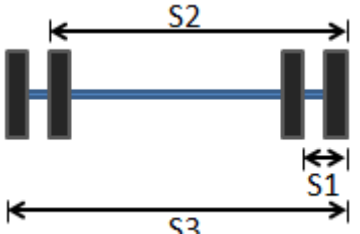
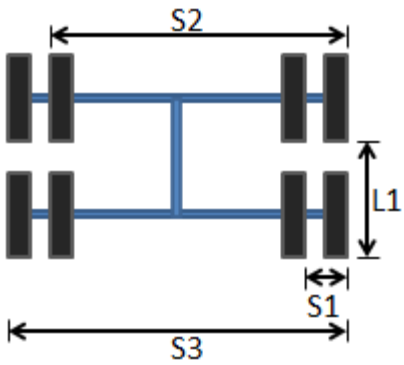
Single Axle		
	Parameter	
	S1	31 cm
	S2	182 cm
	S3	213 cm
	Tire Pressure	8.2 Kg/cm <sup>2</sup>
	Tire Width	25 cm

Table 13: Axle configuration for the tandem axle case

Tandem Axle		
	Parameter	
	S1	31 cm
	S2	182 cm
	S3	213 cm
	L1	145 cm
	Tire Pressure	8.2 Kg/cm <sup>2</sup>
	Tire Width	25 cm

2.3-1.4. Concrete Properties:

Concrete Modulus of Elasticity: To generate different values of radius of relative stiffness (including the minimum and maximum possible values), ISLAB runs with nine different levels of concrete modulus of elasticity were made, see Table 14.

Table 14: Values of modulus of elasticity and corresponding radius of relative stiffness used for ISLAB runs

$E_{PCC}$ (kg/cm <sup>2</sup> )	Radius of relative stiffness (cm)
4,000	18.4186985
10,000	23.1602872
30,000	30.4806522
100,000	41.1854619
300,000	54.2031161
500,000	61.5866303
1,000,000	73.2392589
2,500,000	92.0934925
5,000,000	109.518237

2.3-1.5. Properties of the subgrade:

By using the equivalent structure concept, only one run of the modulus of subgrade reaction ( $k=10$  Kg/cm<sup>3</sup>) needed to be conducted.

### 2.3-1.6. Load Transfer Efficiency

Runs with different levels of load transfer efficiency were made, depending on which joint and the type of cracking considered.

- Pavement/Shoulder Joint
  - 0%
  - 25%
  - 50%
- Transverse Joint:
  - For the transverse cracking case:
    - 50% (because the effect is minimal, only one case was used)
  - For the longitudinal and corner cracking cases: Four different LTE:
    - 10%
    - 30%
    - 50%
    - 80%
- Longitudinal Joint I:
  - 50% (because the effect is minimal, only one case was used)

### 2.3-1.7. Temperature Differential ( $\Delta T_{eff}$ )

To generate different values of Korenev's non-dimensional temperature gradient (including the minimum and maximum possible values), ISLAB runs with nine different levels of temperature differential were conducted, see Table 15.

Table 15: Values of temperature differential and corresponding Korenev's non-dimensional temperature gradient used for ISLAB runs

$\Delta T_{eff}$ (°C)	Korenev's Non-Dimensional Temperature Gradient
-80	-100.1
-50	-62.6
-25	-31.3
-10	-12.5
0	0
10	12.5
20	25.0
40	50.1
65	81.3

## 2.4- Fatigue Algorithm

### 2.4-1. Cracking Model

Cracking is related to fatigue damage by the following relationship:

$$CRK = \frac{1}{1 + C_1 \cdot FD^{-C_2}}$$

The fatigue damage due to all design wheel loads and all traffic increments can be accumulated according to Miner's damage hypothesis by summing the damage over the entire design period using following equation (Miner 1945):

$$FD = \sum \frac{n_{i,j,k,l}}{N_{i,j,k,l}}$$

where:

$FD$  = accumulated fatigue damage over the design period for current crack spacing occurring at the critical fatigue location in the slab.

$n_{ijkl}$  = number of applied axle load applications of the  $j$ th magnitude evaluated during the  $i$ th traffic increment, the  $k$ th temperature difference and the  $l$ th traffic path.

$N_{ijkl}$  = number of allowable axle load applications of the  $j$ th magnitude evaluated during the  $i$ th traffic increment, the  $k$ th temperature difference and the  $l$ th traffic path.

$i$  = axle type

$j$  = load level (incremental load for each axle type)

$k$  = temperature difference

$l$  = traffic path

The maximum bending stresses ( $\sigma_{ij}$ ) and bending strength are used to compute the number of allowable axle load applications ( $N_{ij}$ ) and aggregate interlock wear due to each design wheel load ( $j$ ) for each time increment ( $i$ ) using the following relation:

$$\log(N_{i,j,k,l}) = a \cdot \left( \frac{\sigma_{i,j,k,l}}{MOR \cdot C_1 \cdot C_2} \right)^b$$

Where:

$\sigma_{i,j,k,l}$ : Applied stress, condition  $i,j,k,l$

MOR: Concrete modulus of rupture

a, b: calibration constant; default values: a= 2, b=-1,22

C<sub>1</sub>: Constant due to fracture type

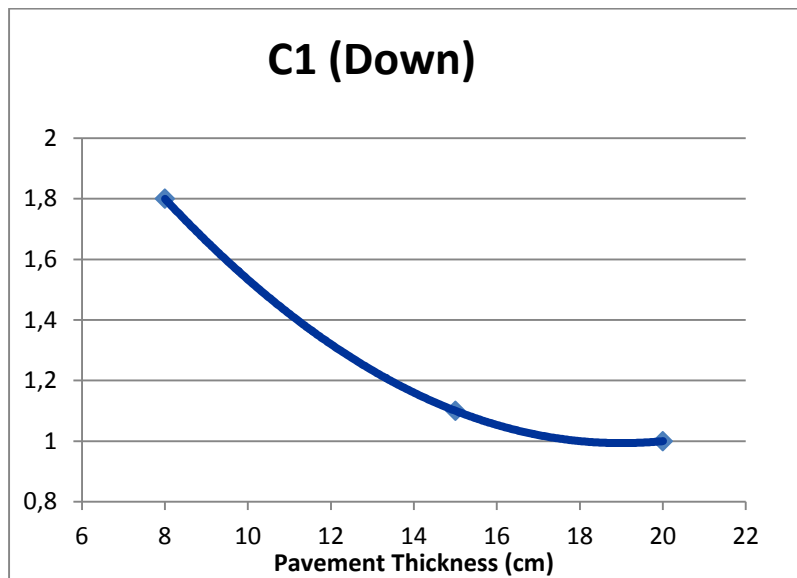


Figure 9: C<sub>1</sub> magnification factor, according to slab thickness

C<sub>2</sub>: Constant for fiber reinforced concrete.

$$C_2 = (1+R_{3,e})$$

$$R_{3,e} = \frac{f_{150}^{150}}{MOR}$$

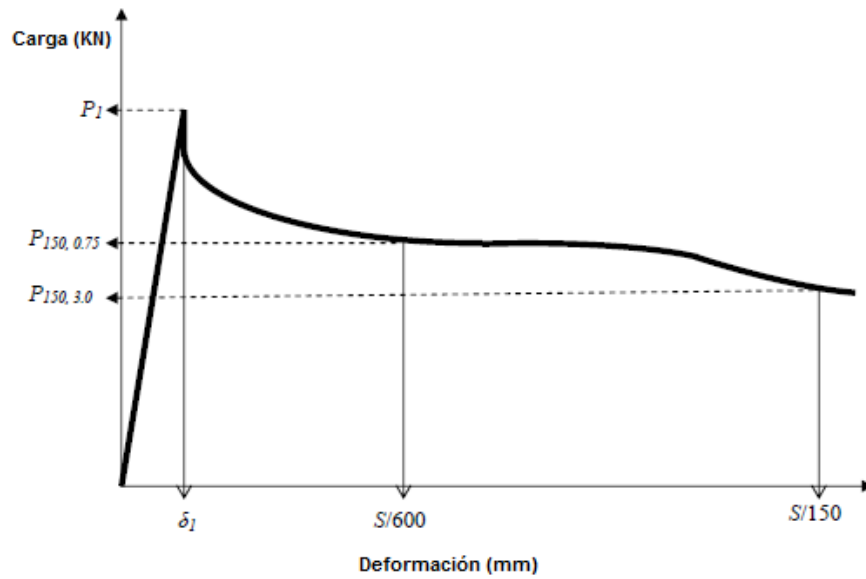


Figure 10: Load deformation curve

Total Cracking at 50% of reliability is determined using the following equation:

$$CRK_{50} = CRK_E + CRK_L + CRK_T - CRK_E \cdot CRK_L - CRK_E \cdot CRK_T - CRK_L \cdot CRK_T + 2 \cdot CRK_E \cdot CRK_L \cdot CRK_T$$

Where

$CRK_{50}$  = Percentage of cracked slabs, 50% of reliability

$CRK_E$  = Percentage of corner cracks

$CRK_L$  = Percentage of longitudinal cracks

$CRK_T$  = Percentage of transverse cracks

Where:

$$CRK_E = \text{Max} (CRK_{Ei})$$

$$CRK_L = \text{Max} (CRK_{Li})$$

#### 2.4-2. Cracking Reliability

The formula to get the level of cracking at a certain level of reliability (m) is:

$$CRK_m = CRK_{50} \cdot Z_r \cdot STD_{CR}$$

$$CRK_m < 100 \%$$

Where:

$CRK_m$  = Percentage of cracked slab at a certain level of reliability (m)

$CRK_{50}$  = Percentage of cracked slabs at 50% level of reliability

$Z_r$  = standard normal deviate for the given reliability level m

$STD_{CR}$  = standard deviation of cracking at the predicted level of mean cracking:

$$STD_{CR} = -0.010229 CRACK^2 + 1.037 CRACK + 3.15$$

### 2.4-3. Effect of Traffic Wander Distribution

The stress produced by the position of the load from the edge/shoulder joint is critical, as shown in Figure 11.

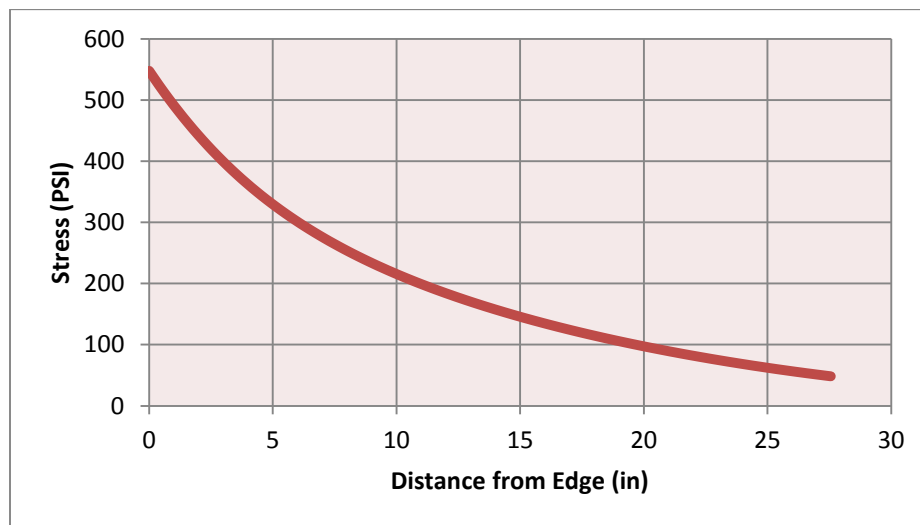


Figure 11: Effect of traffic wander on stress

The position where the trucks wander varies, with a higher percentage on the path, as shown in Figure 12.

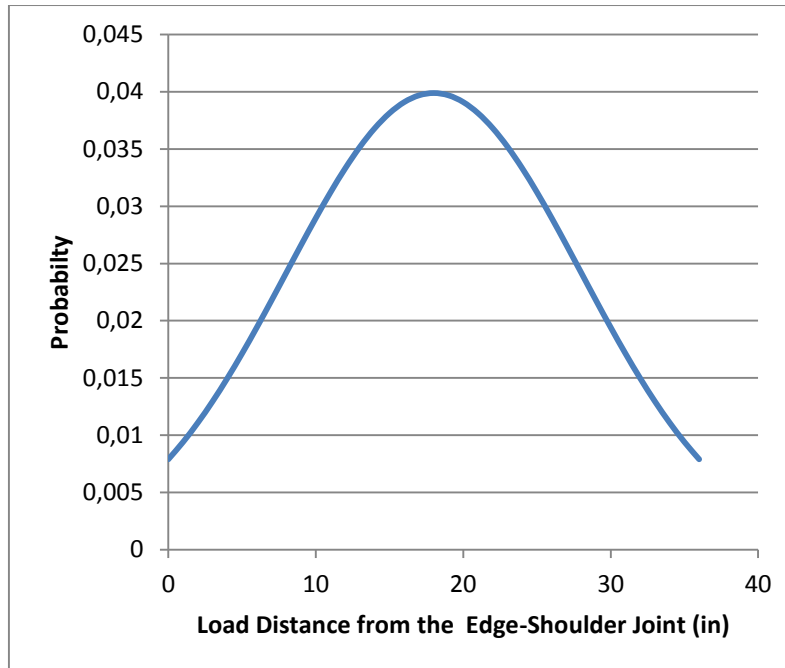


Figure 12: Probability of a truck being located a specific distance from the shoulder joint

Therefore, the stress produced by type of axle  $l$ , load category  $j$  and differential temperature  $k$ ,  $\sigma_{i,j,k}$ , is computed as:

$$\sigma_{i,j,k} = \int_{x=0}^{x=w} \sigma(x)_{i,j,k} \cdot \text{prob}(x) d(x)$$

Where:

X: Load Position

$\sigma(x)_{i,j,k}$ : stress produced by type of axle  $l$ , load category  $j$  and differential temperature  $k$  at position  $x$

$\text{prob}(x)$ : Probability that the load is in position  $x$

$w$ : PCC slab width

This equation can be simplified by dividing the curve in  $n$  rectangles of width  $w_x$  and height  $p_x$ :

$$\sigma_{i,j,k} = \sum_{x=1}^n \sigma(x)_{i,j,k} \cdot w_x \cdot p_x$$

#### 2.4-4. Traffic Wander Model for Bottom Mid-Panel Stress and Top Corner Stress:

The traffic wander model for bottom mid-panel stress and top corner stress considers five different positions. Due to the fact that, in the bottom mid-panel and top corner cases, the stress near the shoulder-edge joint is considerably higher, the five positions are:

- 0 inches from the shoulder-edge joint
- 2 inches from the shoulder-edge joint
- 4 inches from the shoulder-edge joint
- 7.9 inches from the shoulder-edge joint
- 27.6 inches from the shoulder-edge joint

#### 2.4-5. Traffic Wander Model for Bottom Wheel Path Stress

For bottom wheel path stresses, the effect of the wheel path is also important, because the stress is higher when the load is above the evaluation point, and is considerably lower when the load is away from the evaluation point, where the crack may occur. Due to the fact that both tires interact, and thus stresses may difficult to compute correctly with the neural network, a conservative solution was to calculate the maximum stress for the condition when the affected area of the load is over the evaluation point, and to use zero when the affected area of the load is out of the evaluation point area. The three different evaluation areas considered were:

- 13.8 inches from the shoulder-edge joint
- 27.6 inches from the shoulder-edge joint
- 41.4 inches from the shoulder-edge joint

To calculate the probability of the affected area of the load being over one of the evaluation points, the user must define the affected area, which is the distance between the outer edge of one tire and the outer edge of the second tire i.e. two times the tire width ( $T_w$ ) plus the free space between both wheels ( $T_s$ ), as shown in Figure 13:

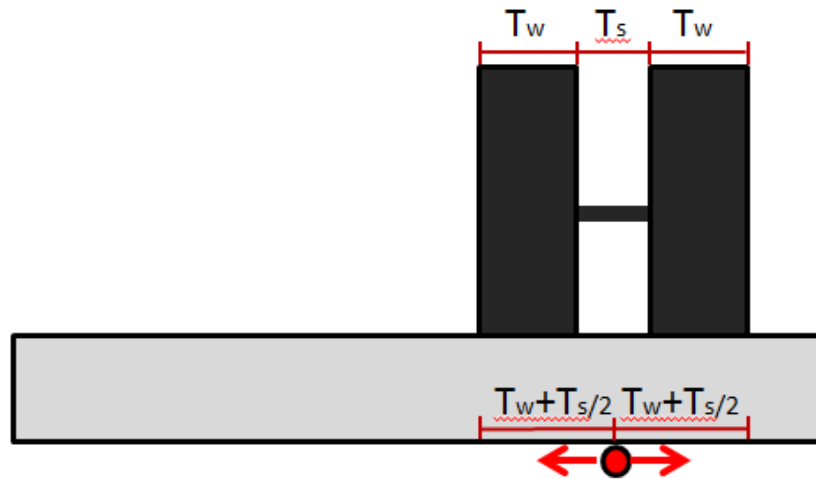


Figure 13: Area affected by a wheel load

The stress produced by type of axle  $l$ , load category  $j$  and differential temperature  $k$  on the evaluation point  $m$   $\sigma_{i,j,k,m}$  for bottom wheel path stress is computed as:

$$\sigma_{i,j,k,m} = \sum_{x=0}^w \text{Max } \sigma_{i,j,k,m}(x) \cdot \text{prob}(x)$$

## 2.4-6. Accounting for Different Axles Types and Cracking Types

### 2.4-6.1. Accounting for Transverse Cracking

For single axles, the critical load case is a single load in the center of the slab see Figure 14.

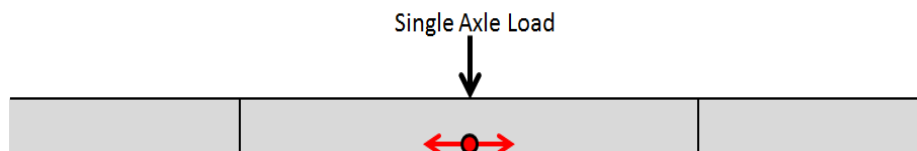


Figure 14: Placement of single axle to determine transverse cracking.

The tandem axle load case is the same as two single axle loads, each with half of the tandem axle load, see Figure 15.

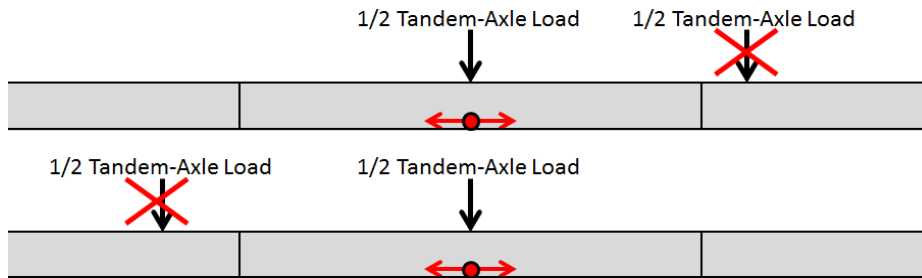


Figure 15: Placement of tandem axles to determine transverse cracking

The tridem axle load case is the same as three single axles, each with a third of the tridem axle load, see Figure 16

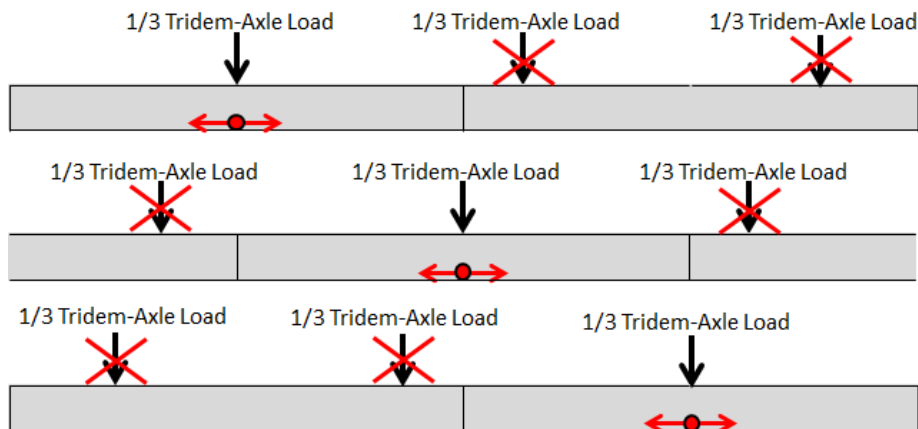


Figure 16: Placement of tridem axles to determine transverse cracking

#### 2.4-6.2. Longitudinal Cracking

The accounting in longitudinal cracking is similar as the transverse cracking, only that the load is placed on the edge of the transverse joint.

For single axles, the critical load case is a single load at the edge of the slab, see Figure 17.

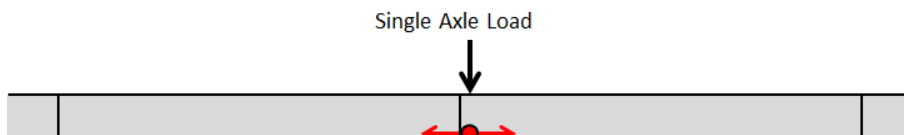


Figure 17: Placement of single axles to determine longitudinal cracking.

The tandem axle load case is the same as two single axle loads, each with half of the tandem axle load, see Figure 18.

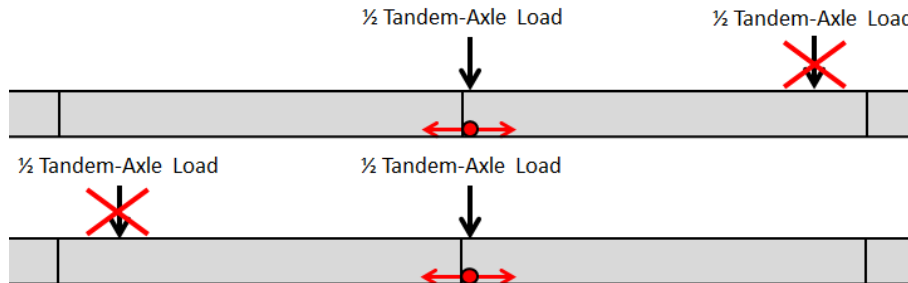


Figure 18: Placement of tandem axles to determine longitudinal cracking

The tridem axle load case is the same as three single axles, each with a third of the tridem axle load, see Figure 19.

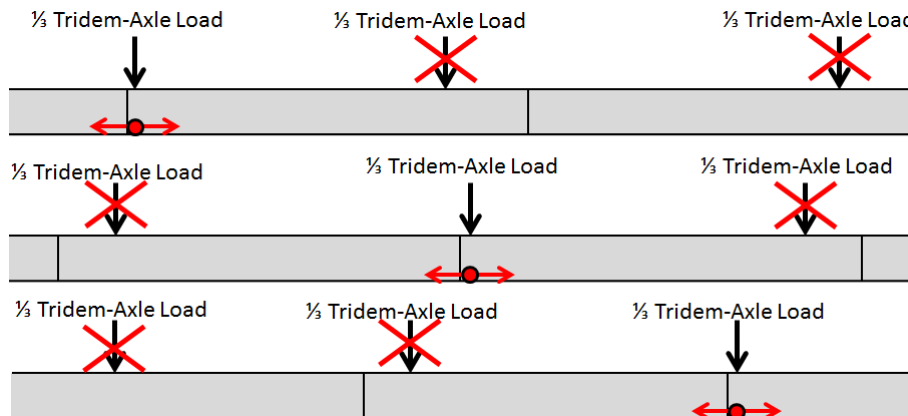


Figure 19: Placement of tridem axles to determine longitudinal cracking.

### 2.4-6.3. Accounting for Corner Cracking

The axle configurations used to determine corner cracking are different than those used to determine transverse and longitudinal cracking. For single loads, the axle is placed on the edge of the transverse joint, see Figure 20.



Figure 20: Placement of single axles to determine corner cracking

In the corner cracking case, tandem axles are not converted to single axles because the stress produced by a tandem axle is considerably higher than the stress of one single axle. One of the tandem axle loads is placed on the edge of the transverse joint, while the other is placed on the slab being considered, see Figure 21. To determine the stresses induced by tandem axles used to predict corner cracking, both the case of a tandem axle loading the slab and a single axle loading the edge of the transverse joint must be considered.

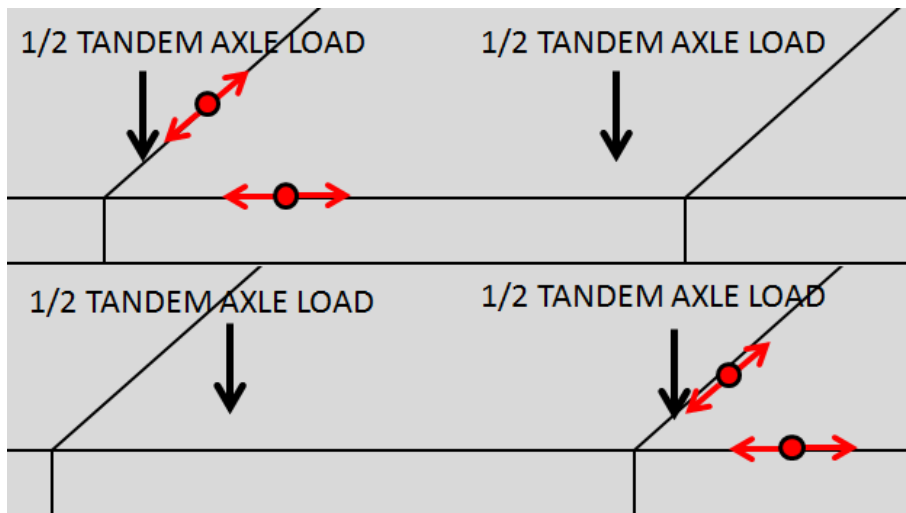


Figure 21: Placement of tandem axles to determine corner cracking

To determine the stresses induced by tridem axles used to predict corner cracking, three cases must be considered. Two of the cases involve a tandem axle loading the slab, and the third is a single axle load on the slab, see Figure 22.

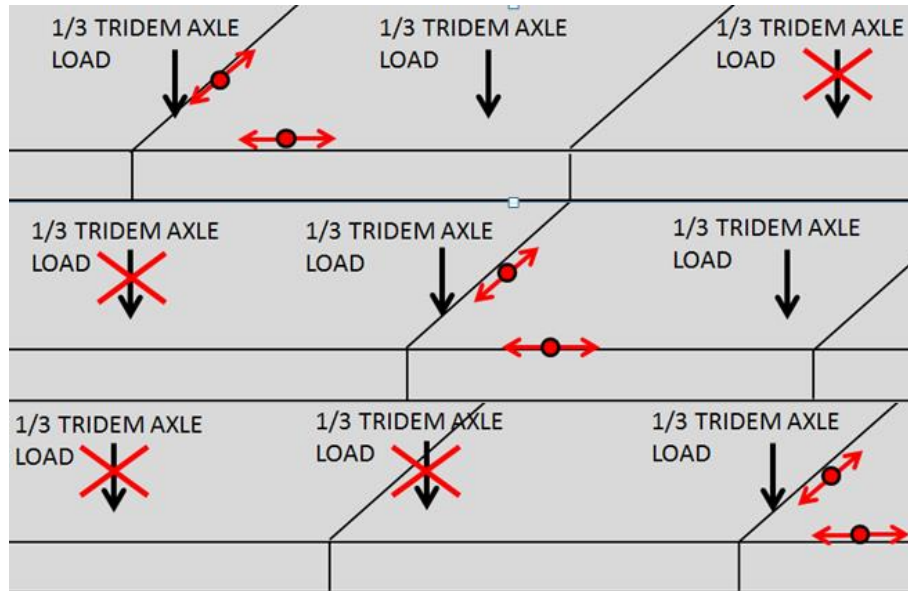


Figure 22: Placement of a tridem axle to determine corner cracking

## 2.5- Load Transfer Efficiency Model

The load transfer efficiency is a function of the joint opening ( $cw$ ):

$$cw = \text{Max}(L \cdot \beta \cdot (\alpha \cdot (T_{\text{constr.}} - T_{\text{media}}) + \epsilon_{\text{horm}}))$$

Where:

$cw$ : Joint opening

$L$ : Joint Spacing

$\beta$ : Pavement-Base Friction coefficient

$\alpha$ : Coefficient of thermal expansion

$T_{\text{constr.}}$ : Concrete Setting Temperature

$T_{\text{promedio}}$ : Mean Temperature

$\epsilon_{\text{horm}}$ : 365-days concrete shrinkage

Due to the fact that the load transfer efficiency is higher in winter than in summer, the joint opening was calculated for summer and winter separately.

The shear capacity of the joint provided by the aggregate is:

$$s = a \cdot (h_{pcc})^b \cdot e^{d \cdot c_w}$$

Where:

a,b,c Calibration Factors: a=0,07, b=1,36 y d=-0,0342

$h_{pcc}$ : Concrete Thickness

$$\text{Log}(agg/kl) = a \cdot e^{-e^{-\left(\frac{J_s-b}{c}\right)}} + d \cdot e^{-e^{-\left(\frac{s-e}{f}\right)}} + g \cdot e^{-e^{-\left(\frac{J_s-b}{c}\right)}} \cdot e^{-e^{-\left(\frac{s-e}{f}\right)}}$$

Where:

a=-4

b=-11.26

c=7.56

d=-28.85

e=0.35

f=0.38

g=56.25

s: shear capacity of the joint provided by the aggregate

$J_s$ : LTE between the pavement and the shoulder

$$x = \log(agg/kl) + 4$$

$$\text{Log}(agg/kl) = \frac{0.15984353 + 0.13029748 \cdot x + 0.01913246 \cdot x^2 - 0.18655878 \cdot x^3 + 0.086967231 \cdot x^4}{(1 - 0.39498611 \cdot x + 0.058358386 \cdot x^2 - 0.0055641051 \cdot x^3 + 0.009554144 \cdot x^4) \cdot 100}$$

## 2.6- Faulting and Load Transfer Efficiency Loss through Energy Differential

The faulting and the load transfer efficiency loss are computed using incremental models based on each semester.

### 2.6-1. Load Transfer Efficiency Loss

Due to load application, the shear capacity of the aggregate of the concrete that provides load transfer efficiency on the joint decreases during time. The next model estimates this loss during each semester.

$$\Delta s_i = 0 \quad \text{if } jw < 0,001 \cdot h_{pcc}$$

$$\Delta s_i = \frac{a \cdot 10^{-6}}{b + c \cdot \left(\frac{jw}{h_{pcc}} - d\right)^f} \left(\frac{\tau_{iA}}{\tau_{ref}}\right) \quad \text{if } jw > 0,001 \cdot h_{pcc}$$

Where:

$h_{pcc}$ : Thickness of the concrete slab

a,b,c,d and f are calibration factors.

$$\tau_{ref} = 111,1 * \exp(-\exp(0,9988 * \exp(-0,1089 * \log(J_{AGG})))$$

- $\tau_{ref}$  = Esfuerzo de corte referencial, derivado de resultados de pruebas de la PCA
- $J_{AGG}$  = Nondimensional stiffnesses of aggregate joint.

$$\tau_i = J_{AGG} * (\delta_{L,i,A} - \delta_{U,i,A})$$

- $\tau_{iA}$ : Shear stress on the transverse joint surface from the response model for the load group i..
- $J_{AGG}$  = Nondimensional stiffnesses of aggregate joint.
- $\delta_{L,i,A}$  = Corner deflections of the loaded slab caused by axle loading of type A and load category i.
- $\delta_{U,i,A}$  = Corner deflections of the unloaded slab caused by axle loading of load category i.

The shear capacity loss of the aggregate on the joint is calculated each semester, by computing every load application during that semester, as show non the next formula:

$$\Delta S_{tot} = \sum_{i=1}^2 \sum_{i=1}^{N_A} \Delta S_{i,A} n_{i,A}$$

Where:

- $\Delta S_{tot}$  = Agregate shear loss accumulated during semester i
- $\Delta S_{i,A}$  = Agregate shear loss produced by axle type A and load category i.
- $N_{i,A}$  = Number of load repetitions of axle type A and load category i

## 2.6-2. Faulting Model

The mean transverse joint faulting is predicted using an incremental approach. A faulting increment is determined each month and the current faulting level affects the magnitude of an increment. The faulting in each month is determined as a sum of faulting increments from all previous months in the pavement life since the opening to traffic using the following model (Khazanovich et al. 2004):

$$\begin{aligned}
 Fault_m &= \sum_{i=1}^m \Delta Fault_i \\
 \Delta Fault_i &= C_{34} * (FAULTMAX_{i-1} - Fault_{i-1})^2 * DE_i \\
 FAULTMAX_i &= FAULTMAX_{i-1} + C_7 * DE_i * \text{Log}(1 + C_5 * 5.0^{EROD})^{C_6} \\
 FAULTMAX_0 &= C_{12} * \delta_{\text{curling}} * \left[ \text{Log}(1 + C_5 * 5.0^{EROD}) * \text{Log}\left(\frac{P_{200} * \text{WetDays}}{P_s}\right) \right]^{C_6}
 \end{aligned}$$

where,

$Fault_m$  = mean joint faulting at the end of semester  $m$ , in.

$\Delta Fault_i$  = incremental change (semiannual) in mean transverse joint faulting during semester  $i$ , in.

$FAULTMAX_i$  = maximum mean transverse joint faulting for semester  $i$ , in.

$FAULTMAX_0$  = initial maximum mean transverse joint faulting, in.

$EROD$  = base/subbase erodibility factor.

$DE_i$  = differential deformation energy accumulated during semester  $i$ .

$EROD$  = base/subbase erodibility factor (see PART 2, Chapter 2).

$\delta_{\text{curling}}$  = maximum mean monthly slab corner upward deflection PCC due to temperature curling and moisture warping.

$P_s$  = overburden on subgrade, lb.

$P_{200}$  = percent subgrade material passing #200 sieve.

$WetDays$  = average annual number of wet days (greater than 0.1 in rainfall).

$C_1$  through  $C_8$  and  $C_{12}$ ,  $C_{34}$  are calibration constants:

$$C_{12} = C_1 + C_2 * FR^{0.25}$$

$$C_{34} = C_3 + C_4 * FR^{0.25}$$

$$C_1 = 1.29$$

$$C_2 = 1.1$$

$$C3 = 0.001725$$

$$C4 = 0.0008$$

$$C5 = 250$$

$$C6 = 0.4$$

$$C_7 = 1.2$$

*FR* = base freezing index defined as percentage of time the top base temperature is below freezing (32 °F) temperature.

## 2.7- IRI Model

The IRI model was calibrated and validated using LTPP (FHWA 2009) and other field data to assure that it would produce valid results under a variety of climatic and field conditions. The final calibrated model is:

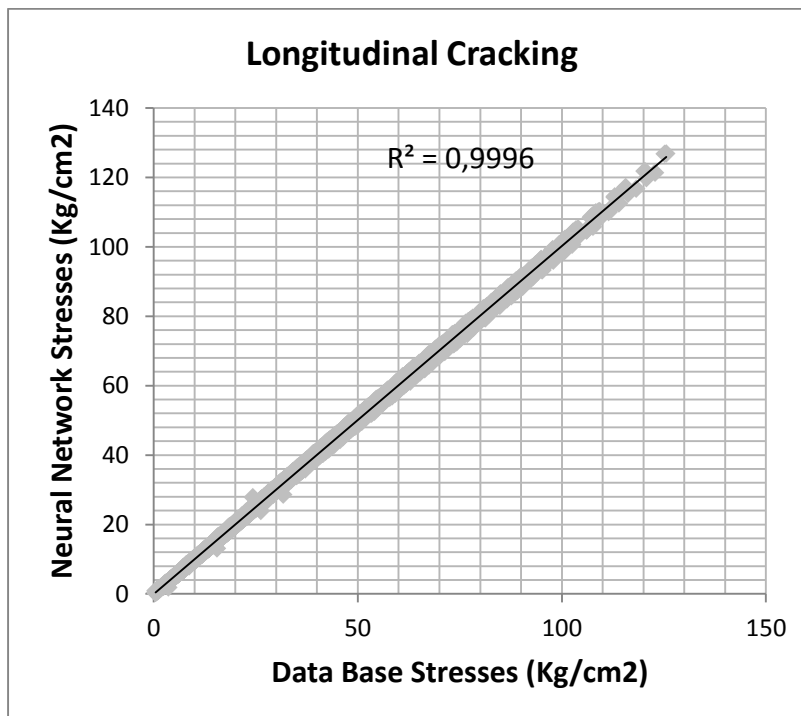
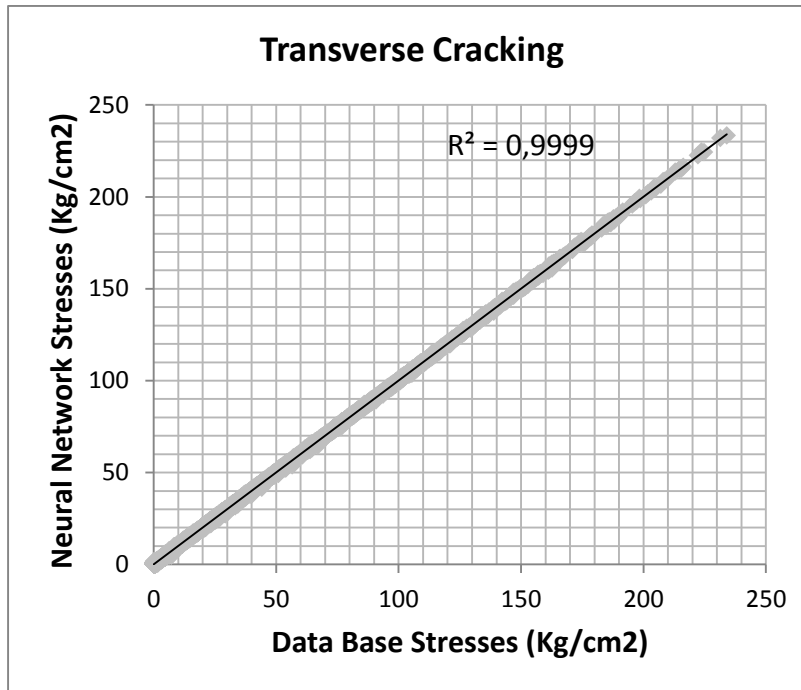
$$IRI = IRI_i + C1 CRK + C2 SPALL + C3 TFAULT + C4 SF$$

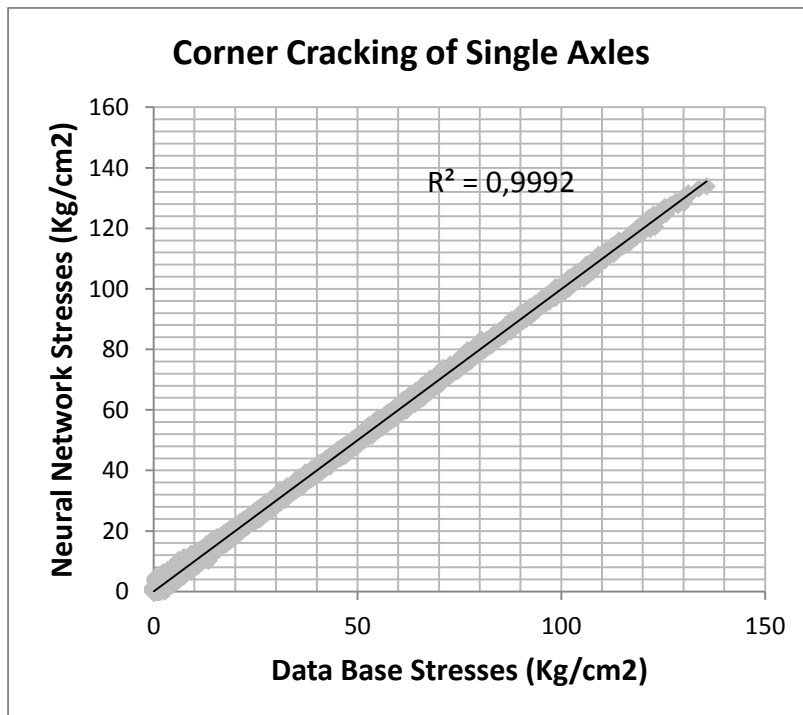
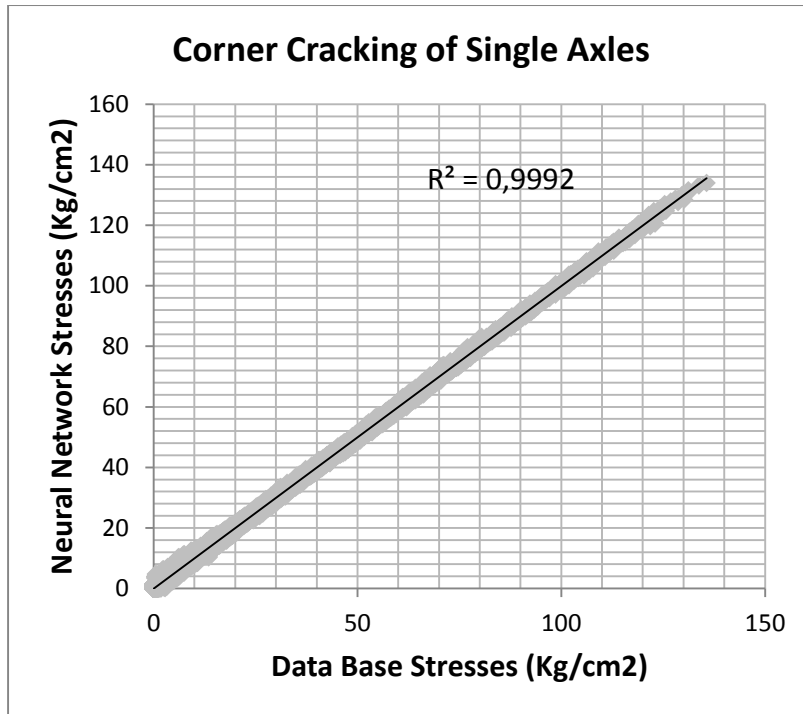
Where:

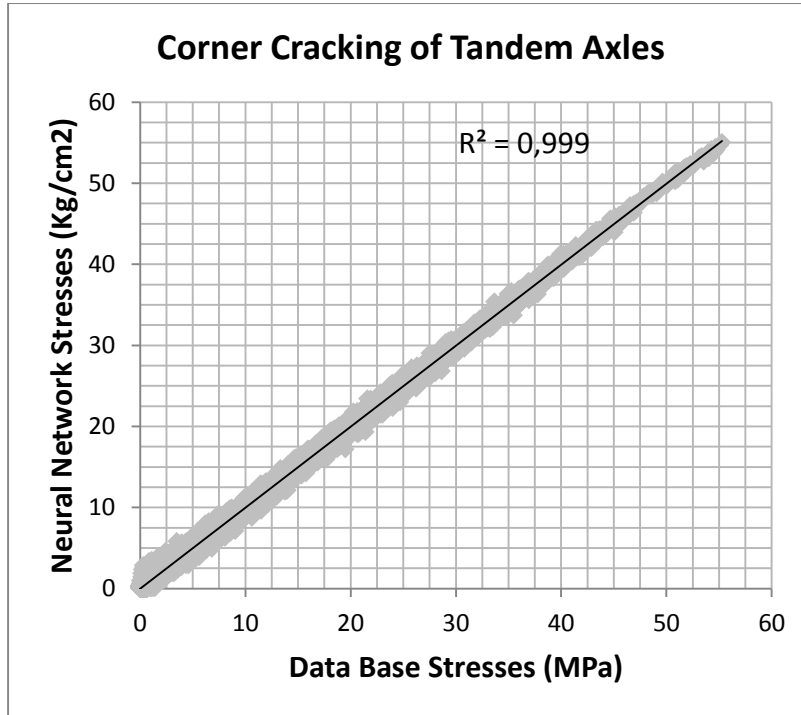
<i>IRI</i>	=	predicted IRI, in/mi.
<i>IRI<sub>i</sub></i>	=	initial smoothness measured as IRI, in/mi.
<i>CRK</i>	=	percent slabs with transverse cracks (all severities).
<i>SPALL</i>	=	percentage of joints with spalling (medium and high severities).
<i>TFAULT</i>	=	total joint faulting cumulated per mi, in.
<i>SF</i>	=	site factor
<i>C1</i>	=	0.0823
<i>C2</i>	=	0.4417
<i>C3</i>	=	1.4929
<i>C4</i>	=	25.24
<i>SF</i>	=	$AGE (1+0.5556 FI) (1+P_{200})/1,000,000$
where,		
<i>AGE</i>	=	pavement age, yr.
<i>FI</i>	=	freezing index, °F-days.
<i>P<sub>200</sub></i>	=	percent subgrade material passing No. 200 sieve.

### 3. Neural Networks Training and Test

#### 3.1- Neural Network Test



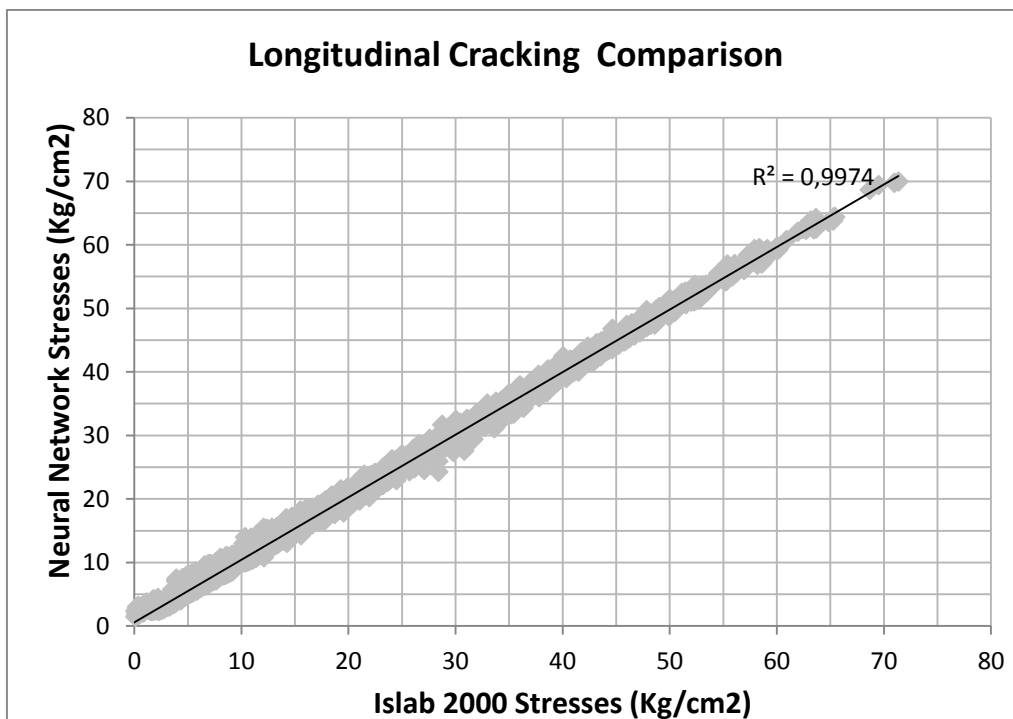
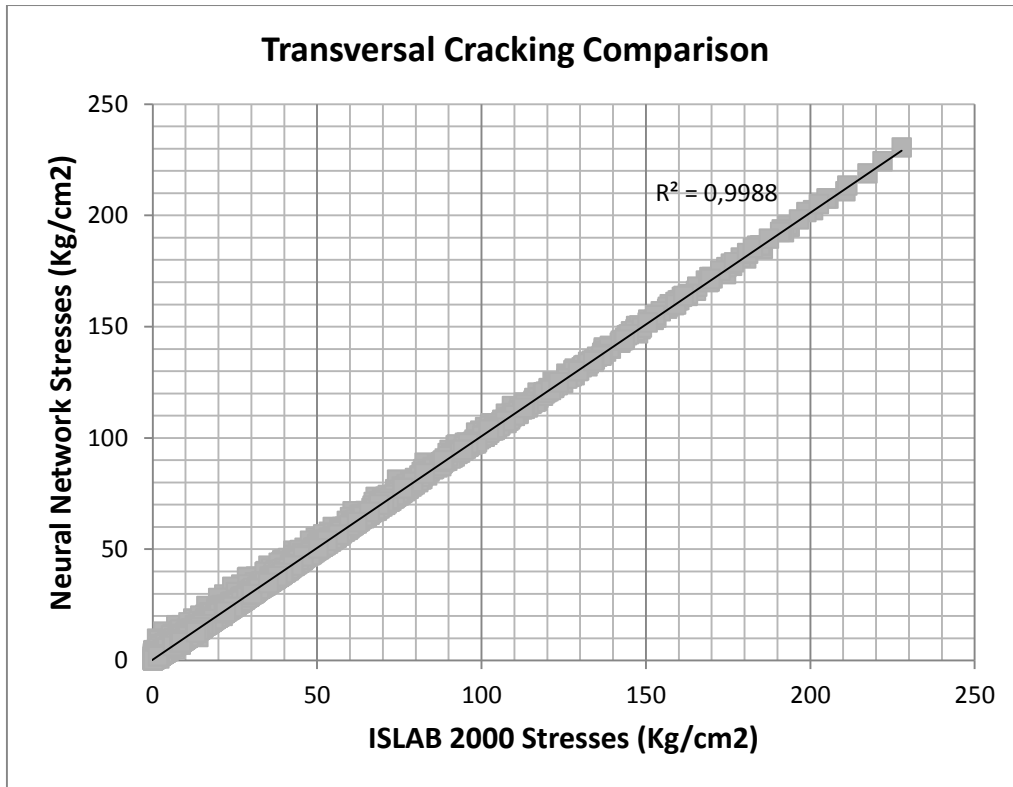


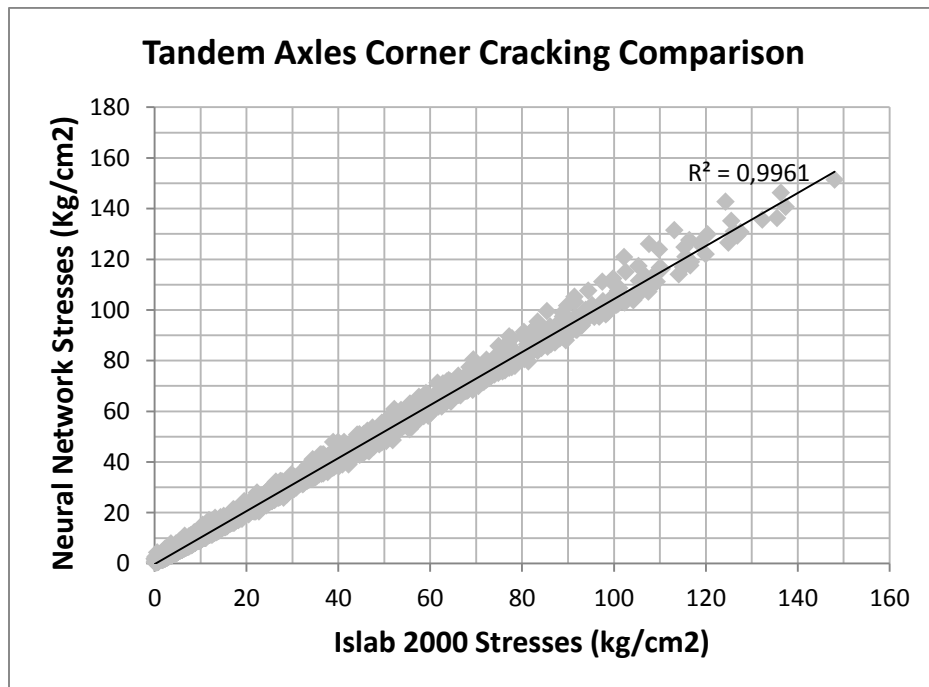
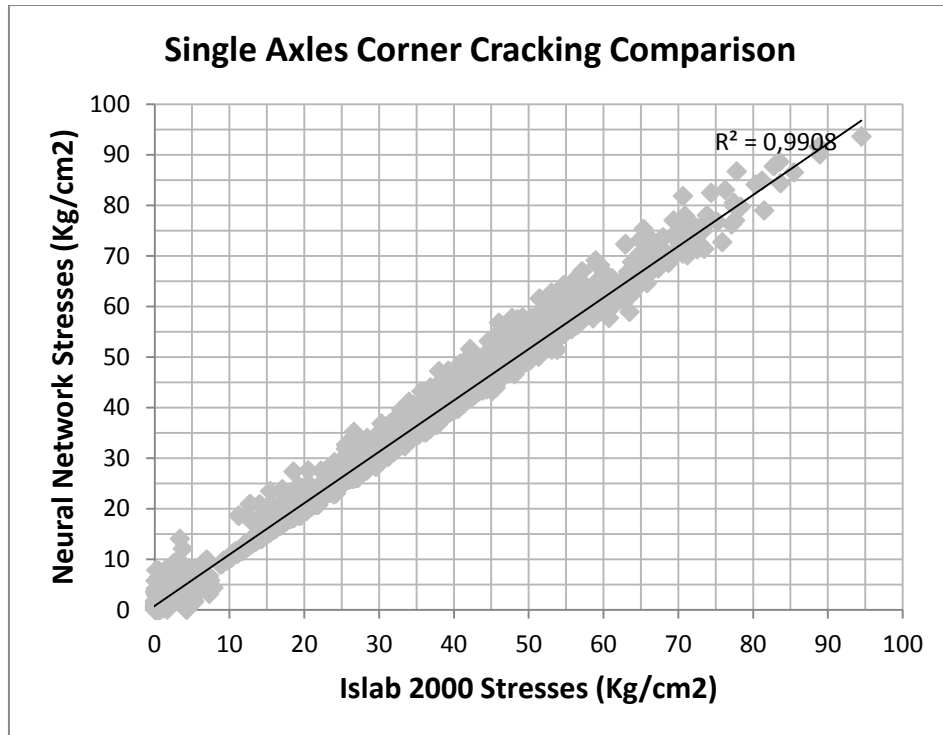


Several cases were made, to check the precision of the neural network versus real cases computed on Islab2000™. In total 4,608 cases were compared.

Table 16: Inputs considered on Islab2000-Neural Network comparison

Espesor Hormigón	Espesor base	k-Subrasante	Diferencial de Temperatura	Transferencia de Carga en el Borde	Posición del Eje	Carga por Eje
6 cm	5 cm	5	-15°C	1%	0 cm	4.000 Kg
10 cm	15 cm	8	-5°C	20%	10 cm	10.000 Kg
15 cm	20 cm	10	0°C		40 cm	16.000Kg
20 cm		20	5°C		65 cm	





## 4. Optipave 2 Calibration

Several different pavement test sections has been developed in recent years to calibrate the design program. First of all the joint opening-load transfer efficiency model must be calibrated in order to calibrate the fatigue damage-percentage of cracked slabs relationship.

### 4.1- Joint Opening-Load transfer efficiency relationship calibration:

This part of the calibration was performed with the data of the accelerated pavement test section, conducted in Illinois and test sections builded in Chile. The load transfer efficiency was measured using the falling weight deflectometer, measuring the deflections in both sides of a joint produced by a falling mass in one of the two sides.

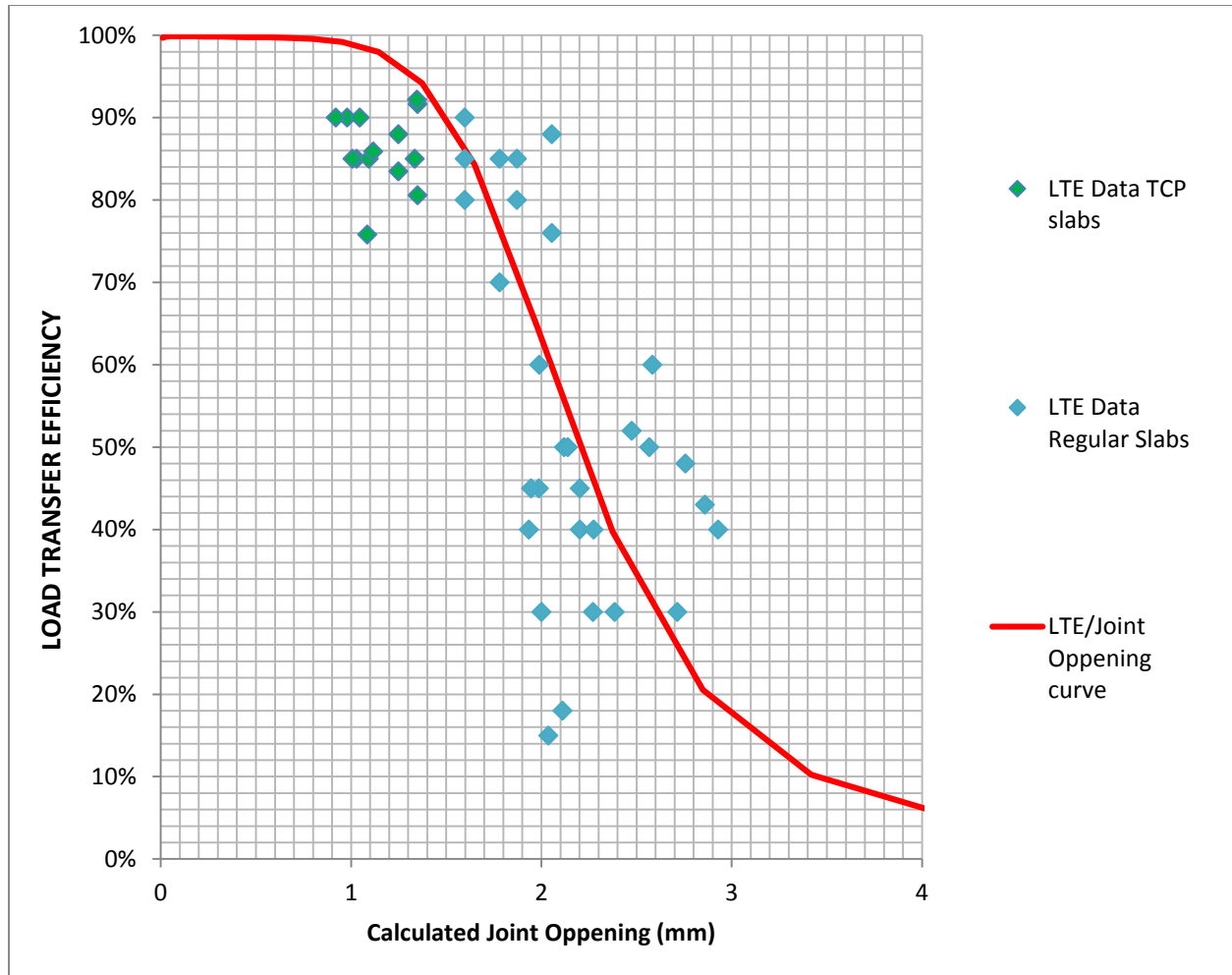
Test Section	Joint opening (mm)	Load Transfer Efficiency (%)
Illinois	0.71	90%
Illinois	0.71	90%
Illinois	0.71	85%
Illinois	0.71	85%
Illinois	0.71	85%
Illinois	0.71	90%
LNV Test Section	0.91	81%
LNV Test Section	0.91	84%
LNV Test Section Gauss	0.91	92%
LNV Test Section Gauss	0.91	92%
LNV Test Section Gauss	0.91	85%
LNV Test Section Gauss	0.91	88%
LNV Test Section Gauss	0.91	86%
LNV Test Section Gauss	0.91	76%
Polpaico-El Trebal Test Section	0.71	90%

Data of pavements with regular size were also included in this part of the calibration.

Test Section	Joint opening (mm)	Load Transfer Efficiency (%)
Longotoma	1,62	30%
Lampa	1,37	30%
Lampa	1,37	40%
Lampa	1,37	45%
Lampa	1,37	50%
Lo Vásquez	1,37	30%
Lo Vasquez	1,37	40%
Lo Vásquez	1,37	18%

<b>Lo Vásquez</b>	1,37	30%
<b>Talagante</b>	1,37	50%
<b>Talagante</b>	1,37	60%
<b>Talagante</b>	1,37	40%
<b>Paine</b>	1,72	40%
<b>Paine</b>	1,72	43%
<b>Paine</b>	1,72	48%
<b>Paine</b>	1,72	60%
<b>Graneros</b>	1,38	45%
<b>Graneros</b>	1,38	45%
<b>San Fernando</b>	1,54	50%
<b>San Fernando</b>	1,54	52%
<b>Melipilla</b>	1,37	15%
<b>Melipilla</b>	1,36	80%
<b>Melipilla</b>	1,37	85%
<b>Melipilla</b>	1,36	90%
<b>Melipilla</b>	1,37	80%
<b>Melipilla</b>	1,36	85%
<b>Leyda</b>	1,37	88%
<b>Leyda</b>	1,37	70%
<b>Leyda</b>	1,37	76%
<b>Leyda</b>	1,37	85%

First the error between the load transfer efficiency model and the measured load transfer efficiency was calculated. Then coefficient a,b and d of the aggregate shear joint capacity V/S joint opening relationship were adjusted to get the minimum sum of total error. Finally the solution curve was plotted with the measured data and a curve with a safety factor was also added.



**4.2- Cracking Model Calibration:**

The next step was to calibrate the relationship between fatigue damage calculated by the software and the percentage of cracked slabs. For this purpose data of different test sections was compiled.

4.2-1. Test sections conducted by the Cement and Concrete Institute of Chile

Three test sections with TCP technology were developed on 2004, 2005 and 2006. The main characteristics of this three test sections are presented on the table above:

Test Section ID	Location	Construction Year	Pavement Thickness
Alameda Calzada Norte	Santiago, Chile	2004	13, 16 y 20 cm
Chiniquihue	10 <sup>th</sup> Region Chile	2005	8, 10 y 12 cm

Padre Las Casas	9 <sup>th</sup> Region Chile	2006	8, 10 y 12 cm
-----------------	------------------------------	------	---------------

Each of this test sections were inspected periodically for a period up to six years. The pavement was checked for cracks on their slabs in each inspection. The results of this tests are presented on the next table:

Table 1: Results of Alameda Calzada Norte Test Section

Subsection N°	Inspection N°	Pavement Thickness (mm)	Accumulated Essals	Percentage of Cracked Slabs		
				Transversal Crack	Longitudinal Crack	Corner Crack
1	1	152	10.552.195	42%	4%	0%
	2	152	15.891.912	24%	2%	0%
2	1	152	10.552.195	42%	4%	0%
	2	152	15.891.912	24%	2%	0%
3	1	152	10.552.195	42%	4%	0%
	2	152	15.891.912	24%	2%	0%
4	1	143	17.586.992	86%	14%	0%
	2	143	26.486.520	72%	8%	0%
5	1	143	17.586.992	86%	14%	0%
	2	143	26.486.520	72%	8%	0%
6	1	143	1.954.110	0%	1%	0%
	2	143	2.942.947	0%	0%	0%
7	1	147	10.552.195	57%	5%	0%
	2	147	15.891.912	37%	3%	0%
8	1	147	10.552.195	57%	5%	0%
	2	147	15.891.912	37%	3%	0%
9	1	147	10.552.195	57%	5%	0%
	2	147	15.891.912	37%	3%	0%
10	1	143	17.586.992	86%	14%	0%
	2	143	26.486.520	72%	8%	0%
11	1	143	17.586.992	86%	14%	0%
	2	143	26.486.520	72%	8%	0%
12	1	143	17.586.992	94%	12%	0%
	2	143	26.486.520	87%	7%	0%
13	1	196	10.552.195	0%	0%	0%
	2	196	15.891.912	0%	0%	0%
14	1	196	1.172.466	0%	0%	0%
	2	196	1.765.768	0%	0%	0%

15	1	196	10.552.195	0%	0%	0%
	2	196	15.891.912	0%	0%	0%
16	1	131	17.586.992	96%	30%	1%
	2	131	26.486.520	91%	19%	0%
17	1	131	1.954.110	24%	2%	0%
	2	131	2.942.947	12%	1%	0%
18	1	131	17.586.992	26%	29%	0%
	2	131	26.486.520	14%	19%	0%
19	1	165	17.586.992	28%	2%	0%
	2	165	26.486.520	15%	1%	0%
20	1	165	1.954.110	0%	0%	0%
	2	165	2.942.947	0%	0%	0%
	3	165	17.586.992	0%	3%	0%
	4	165	26.486.520	0%	2%	0%
21	1	165	1.954.110	28%	2%	0%
	2	165	2.942.947	15%	1%	0%
22	1	165	17.586.992	0%	0%	0%
	2	165	26.486.520	0%	0%	0%
23	1	165	17.586.992	49%	2%	0%
	2	165	26.486.520	30%	1%	0%

Table 2: Results of Chiquihue Test Section

Subsection N°	Inspection N°	Pavement Thickness (mm)	Accumulated Essals	Percentage of Cracked Slabs		
				Transversal Crack	Grieta Longitudinal	Grieta de Esquina
1	1	120	5.401	0%	0%	0%
	2	120	27.487	0%	0%	0%
	3	120	53.850	0%	0%	0%
	4	120	96.194	1%	1%	0%
	5	120	105.028	1%	1%	0%
	6	120	133.559	2%	1%	0%
	7	120	213.408	5%	2%	0%
2	1	120	3.574	0%	0%	0%
	2	120	25.660	0%	0%	0%
	3	120	52.022	0%	0%	0%
	4	120	94.366	1%	1%	0%
	5	120	103.201	1%	1%	0%
	6	120	131.731	2%	1%	0%
	7	120	211.580	5%	2%	0%
3	1	100	1.547	0%	0%	0%

	2	100	5.401	0%	0%	0%
	3	100	27.487	1%	1%	0%
	4	100	53.850	3%	2%	0%
	5	100	96.194	9%	5%	1%
	6	100	133.559	17%	7%	2%
	7	100	213.408	34%	13%	5%
	4	1	100	3.574	0%	0%
2		100	25.660	1%	1%	0%
3		100	52.022	3%	2%	0%
4		100	94.366	9%	5%	1%
5		100	131.731	16%	7%	2%
5	1	80	1.547	0%	0%	0%
	2	80	5.401	1%	1%	2%
	3	80	27.487	9%	7%	23%
	4	80	53.850	26%	15%	53%
	5	80	96.194	53%	29%	78%
	6	80	133.559	68%	38%	87%

Table 3: Results of Padre Las Casas Test Section

Subsection N°	Inspection N°	Pavement Thickness (mm)	Accumulated Essals	Percentage of Cracked Slabs		
				Transversal Crack	Grieta Longitudinal	Grieta de Esquina
1	1	120	5.160	0%	0%	0%
	2	120	33.170	1%	0%	0%
	3	120	78.806	4%	4%	0%
	4	120	148.222	13%	9%	0%
	5	120	221.484	24%	15%	0%
	6	120	307.597	38%	21%	0%
2	1	100	5.160	1%	0%	0%
	2	100	33.170	10%	1%	0%
	3	100	78.806	37%	20%	4%
	4	100	148.222	67%	36%	14%
	5	100	221.484	82%	50%	26%
	6	100	307.597	90%	61%	40%
3	1	100	5.160	0%	0%	0%
	2	100	33.170	4%	1%	0%
	3	100	78.806	21%	18%	3%
	4	100	148.222	48%	34%	10%
	5	100	221.484	67%	47%	20%
	6	100	307.597	79%	58%	32%

4	1	120	19.934	0%	0%	0%
	2	120	70.954	3%	4%	0%
	3	120	140.370	11%	9%	0%
	4	120	213.632	23%	14%	0%
	5	120	299.745	37%	21%	0%
5	1	80	5.160	3%	1%	2%
	2	80	33.170	28%	4%	20%
	3	80	78.806	69%	42%	81%
	4	80	148.222	88%	63%	94%
	5	80	221.484	94%	74%	97%
	6	80	307.597	97%	82%	98%
6	1	80	19.934	6%	2%	7%
	2	80	70.954	44%	38%	76%
	3	80	140.370	75%	61%	92%
	4	80	213.632	87%	73%	97%

#### 4.2-2. Additional Test Sections

Between the years 2011 and 2013 several different test sections were built.

Test Section	Location	Year of Construction	Pavement Thickness
Lampa	Santiago Chile	2012	8 and 10 cm FRC
Concrete Plant	Santiago Chile	2012	6 and 8 cm FRC
Los Andes University	Santiago Chile	2011	8 cm FRC
Route 5 Slabs Replacement	VII Regon Chile	2008	16 cm
El Trebal	Santiago Chile	2013	6 y 8 cm FRC

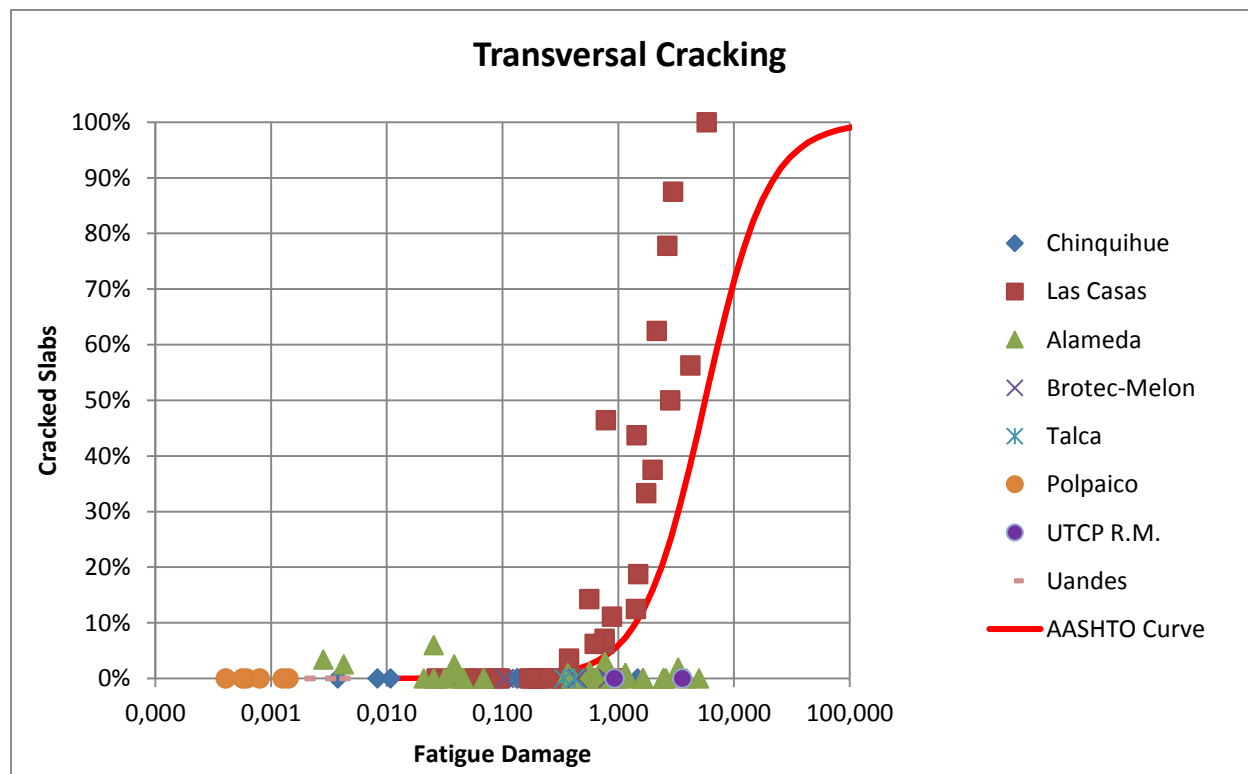
The result of this test sections are shown in the table below:

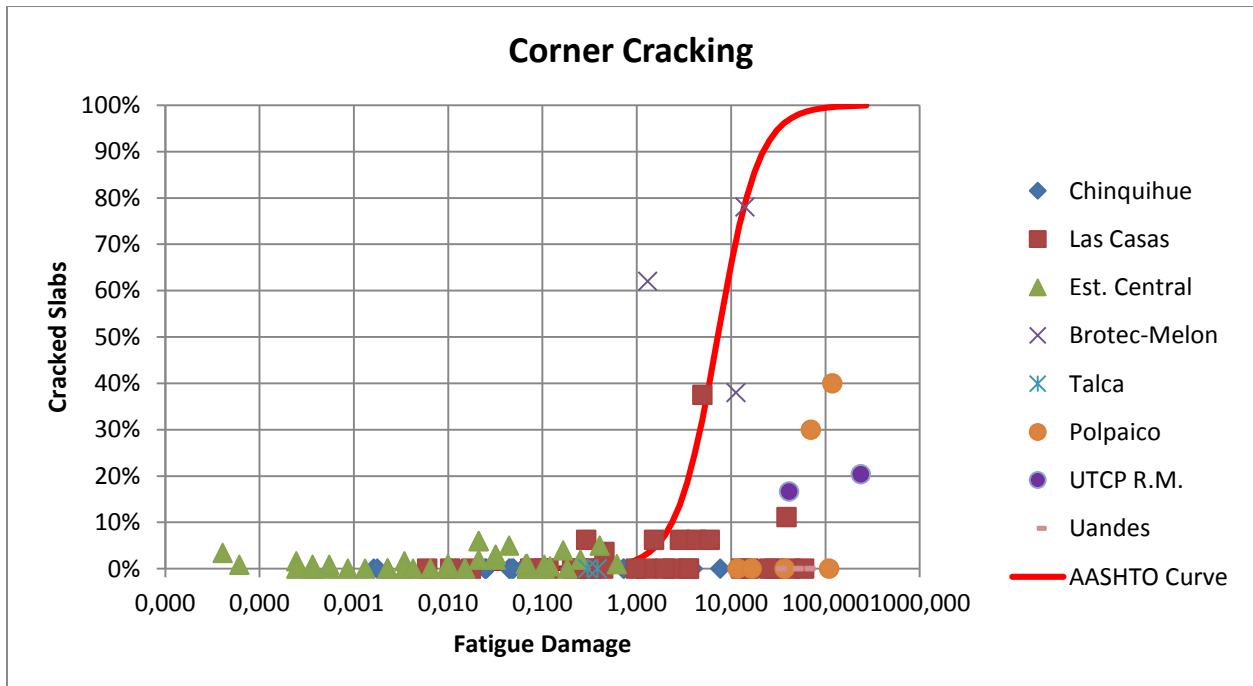
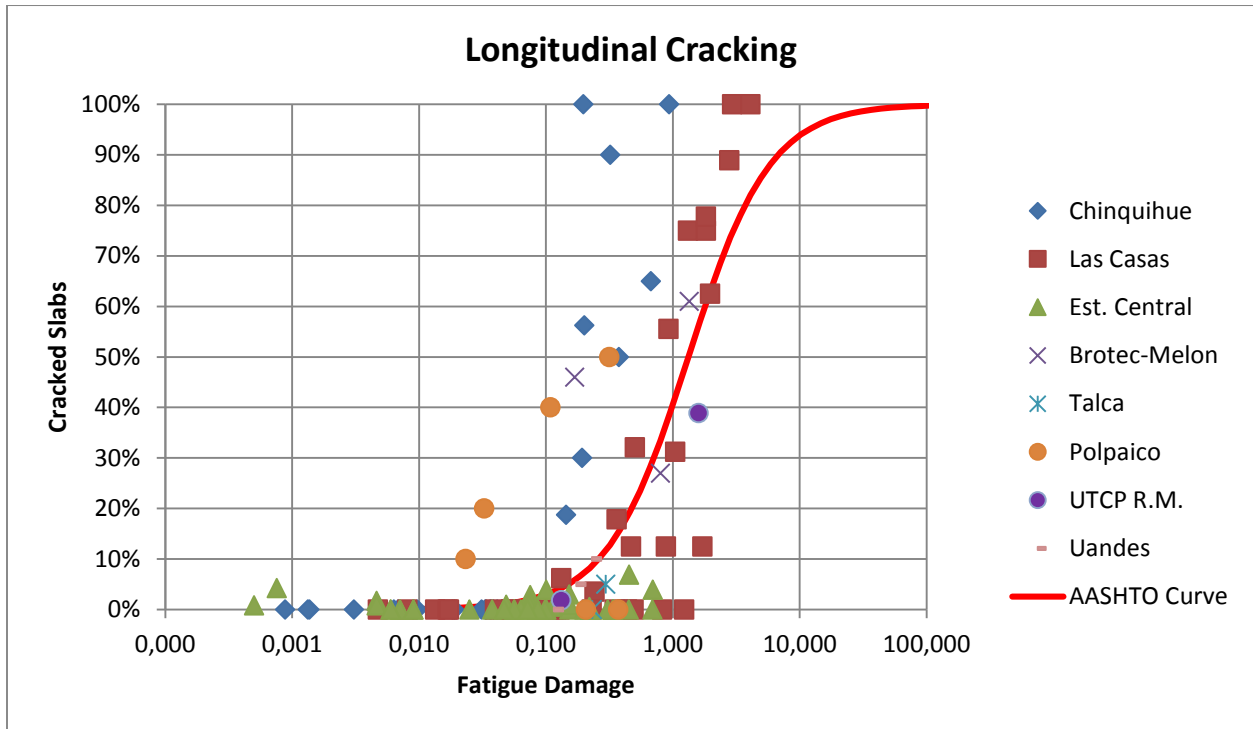
Test Section ID	Subsection	Inspection N°	Pavement Thickness (mm)	Accumulated Essals	Percentage of Cracked Slabs		
					Transversal Crack	Transversal Crack	Transversal Crack
Lampa	1	1	80 FRC	27.348	40%	50%	79%
Lampa	2	1	100 FRC	27.348	1%	6%	3%
Lampa	3	1	80 FRC	27.348	17%	34%	71%
Ruta 5	1	1	160	12.000.000	10%	9%	0%
Ruta 5	1	2	160	15.000.000	15%	12%	0%
El Trebal	1	1	60 FRC	2.087	0%	3%	96%
El Trebal		2	60 FRC	4.884	0%	13%	100%
El Trebal		3	60 FRC	7.119	0%	8%	99%

El Trebal		4	60 FRC	8.488	0%	15%	100%
El Trebal	2	1	80 FRC	8.488	0%	0%	72%
El Trebal		2	80 FRC	11.921	0%	1%	84%
Ready-Mix	1	1	60 FRC	30.000	93%	56%	100%
Ready-Mix	2	1	80 FRC	30.000	46%	4%	97%
Uandes	1	1	80 FRC	36.500	0%	4%	95%
Uandes		2	80 FRC	54.750	0%	6%	97%
Uandes		3	80 FRC	73.000	0%	9%	99%

Each one of the test sections were computed in OptiPave 2, to calculate the fatigue damage during time. After that the total error between the percentage of cracked slabs predicted by the cracking model and the cracked slabs observed in field were calculated. After that, coefficient c1 and c2 of the fatigue damage-percentage of cracked slabs relationship were adjusted to get the minimum sum of total error. This procedure was done for the three types of cracking (transversal, longitudinal and corner cracking). The obtained values of coefficient c1 and c2 are shown on the table below:

Type of Cracking	C1 coefficient	C2 coefficient
Transversal	-1,6	15,75
Longitudinal	-1,35	1,46
Corner	-1,98	50





*\*Software output (red line) was deliberately moved to the left to be conservative (Will predict more cracking than observed). This is because of the small amount of corner cracking observed in the test sections, and the difficulty to predict corner stresses.*

## 5. Supplemental Information

### 5.1- Type of Traffic

The federal highway administration classifies the vehicles among 13 different types, see Figure 23

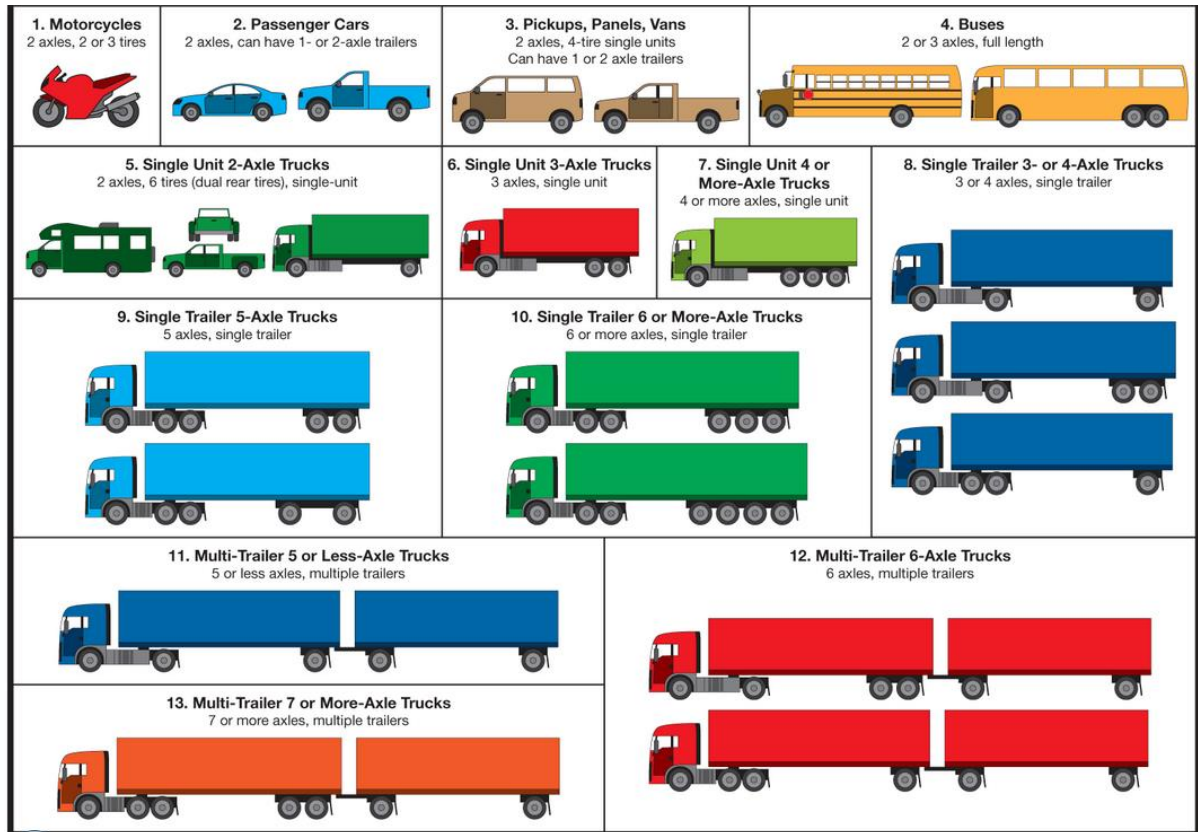


Figure 23: FHWA vehicle classifications

Vehicles types 1 through 3 are light vehicles and therefore are not considered. These 10 types of trucks (classes 4 through 12) are then distributed according to the type of road using Table 17:

Table 17: Vehicle class distribution

TTC Group	TTC Description	Vehicle/Truck Class Distribution (percent)									
		4	5	6	7	8	9	10	11	12	13
1	Major single-trailer truck route (type I)	1,3	8,5	2,8	0,3	7,6	74,0	1,2	3,4	0,6	0,3
2	Major single-trailer truck route (Type II)	2,4	14,1	4,5	0,7	7,9	66,3	1,4	2,2	0,3	0,2
3	Major single- and multi- trailer truck route (Type I)	0,9	11,6	3,6	0,2	6,7	62,0	4,8	2,6	1,4	6,2
4	Major single-trailer truck route (Type III)	2,4	22,7	5,7	1,4	8,1	55,5	1,7	2,2	0,2	0,4

5	Major single- and multi- trailer truck route (Type II).	0.9	14.2	3.5	0.6	6.9	54.0	5.0	2.7	1.2	11.0
6	Intermediate light and single-trailer truck route (I)	2.8	31.0	7.3	0.8	9.3	44.8	2.3	1.0	0.4	0.3
7	Major mixed truck route (Type I)	1.0	23.8	4.2	0.5	10.2	42.2	5.8	2.6	1.3	8.4
8	Major multi-trailer truck route (Type I)	1.7	19.3	4.6	0.9	6.7	44.8	6.0	2.6	1.6	11.8
9	Intermediate light and single-trailer truck route (II)	3.3	34.0	11.7	1.6	9.9	36.2	1.0	1.8	0.2	0.3
10	Major mixed truck route (Type II)	0.8	30.8	6.9	0.1	7.8	37.5	3.7	1.2	4.5	6.7
11	Major multi-trailer truck route (Type II)	1.8	24.6	7.6	0.5	5.0	31.3	9.8	0.8	3.3	15.3
12	Intermediate light and single-trailer truck route (III)	3.9	40.8	11.7	1.5	12.2	25.0	2.7	0.6	0.3	1.3
13	Major mixed truck route (Type III)	0.8	33.6	6.2	0.1	7.9	26.0	10.5	1.4	3.2	10.3
14	Major light truck route (Type I)	2.9	56.9	10.4	3.7	9.2	15.3	0.6	0.3	0.4	0.3
15	Major light truck route (Type II)	1.8	56.5	8.5	1.8	6.2	14.1	5.4	0.0	0.0	5.7
16	Major light and multi-trailer truck route	1.3	48.4	10.8	1.9	6.7	13.4	4.3	0.5	0.1	12.6
17	Major bus route	36.2	14.6	13.4	0.5	14.6	17.8	0.5	0.8	0.1	1.5

Table 18: Single-axle load distribution default values (percentages) for each vehicle/truck class.

	5.1-1. Vehicle/Truck Class									
Axle Load (Lbs)	4	5	6	7	8	9	10	11	12	13
4,500	9,66	50,31	11,65	7,81	31,78	9,48	10,62	16,92	19,7	20,59
8,550	40,57	30,42	40,62	21,66	36,14	44,68	44,69	31,06	34,34	33,17
12,360	31,26	12,47	33,45	31,4	19,02	37,93	36,95	28,63	28,12	32,92
16,410	11,86	4,31	8,75	24,91	8,28	5,43	5,68	15,7	12,74	8,52
20,460	4,54	1,54	3,02	9,35	3,29	1,89	1,33	5,72	3,74	2,85
24,280	1,42	0,59	1,01	3,25	0,97	0,44	0,46	1,39	0,9	1,13
28,325	0,45	0,2	0,34	0,68	0,28	0,1	0,1	0,43	0,31	0,58
32,370	0,15	0,08	0,11	0,84	0,19	0,04	0,07	0,09	0,06	0,21
36,420	0,05	0,06	0,04	0,06	0,04	0,01	0,04	0,04	0,04	0,04
40,015	0,02	0	0,02	0,02	0,01	0	0,05	0,03	0	0,01

Table 19: Tandem-axle load distribution default values (percentages) for each vehicle/truck class

	Vehicle/Truck Class									
Axle Load (Lbs)	4	5	6	7	8	9	10	11	12	13
<b>9,000</b>	11,99	62,03	33,5	30,4	50,07	20,82	13,69	24,53	16,22	21,5
<b>17,100</b>	28,12	18,86	28,03	21,44	30,85	26,15	28,01	29,9	37,7	20,7
<b>24,720</b>	45,56	8,08	19,36	17,61	11,41	21,02	24,91	21,23	29,09	21,19
<b>32,820</b>	11,37	7,6	10,98	12,09	4,77	22,6	20,78	18,57	11,49	20,37
<b>40,920</b>	2,11	2,6	4,54	8,26	1,76	7,61	7,98	4,47	3,48	11,47
<b>48,560</b>	0,56	0,6	2,22	6,26	0,86	1,41	3,24	0,81	1,1	3,11
<b>56,650</b>	0,15	0,16	0,94	2,64	0,16	0,27	0,94	0,4	0,58	1,12
<b>64,740</b>	0,14	0,03	0,34	0,93	0,02	0,08	0,28	0,09	0,19	0,32
<b>72,840</b>	0,01	0,03	0,11	0,31	0	0,03	0,17	0	0,15	0,11
<b>80,030</b>	0	0	0	0,04	0	0	0,01	0	0,01	0,1

Table 20: Tridem-axle load distribution default values (percentages) for each vehicle/truck class.

	Vehicle/Truck Class									
Axle Load (Lbs)	4	5	6	7	8	9	10	11	12	13
<b>13,500</b>	66,67	49,79	46,31	11,39	26,56	80,11	33,02	60,08	26,4	20,01
<b>25,650</b>	0	4,01	18,63	10,51	12,29	11,16	16,68	20,41	14,9	11,52
<b>37,080</b>	0	20,12	12,56	16,6	14,04	4,19	17,49	7,08	19,87	15,32
<b>49,230</b>	33,33	7,11	5,71	21,16	13,52	1,98	18,75	6,03	20,82	17,21
<b>61,380</b>	0	9,59	5,27	18,67	15,92	1,09	9,15	3,86	11,51	16,99
<b>72,840</b>	0	0	2,19	14,19	9,61	0,67	2,92	0,97	2,83	9,4
<b>84,975</b>	0	6,25	6,37	5,51	4,15	0,47	1,21	1,57	1,88	5,03
<b>97,110</b>	0	0	1,49	1,37	3,53	0,21	0,52	0	0,51	2,85
<b>109,260</b>	0	3,13	0,45	0,45	0,21	0,08	0,18	0	0,57	1,07

120,045	0	0	1,02	0,15	0,17	0,04	0,08	0	0,71	0,6
---------	---	---	------	------	------	------	------	---	------	-----

Table 21: Mean default values for the average number of single, tandem, and tridem axles per truck class

TTC Group	Single-Axles	Tandem-Axles	Tridem-Axles
4	1,62	0,39	0,00
5	2,00	0,00	0,00
6	1,02	0,99	0,00
7	1,00	0,26	0,83
8	2,38	0,67	0,00
9	1,13	1,93	0,00
10	1,19	1,09	0,89
11	4,29	0,26	0,06
12	3,52	1,14	0,06
13	2,15	2,13	0,35

Table 22: Load spectra distribution for single axles

Axle Load (Lbs)	Single Axles each 1000 vehicles																
	1	2	3	4	5	6	7	8	9	10	11	12	13	14	15	16	17
4,500	26 0	30 3	30 2	38 2	34 2	45 8	44 1	39 1	49 3	49 3	44 0	56 6	52 6	68 5	67 7	63 4	36 3
8,550	57 3	56 6	58 4	57 4	59 6	57 8	61 2	60 3	58 2	61 6	60 7	59 2	62 1	58 7	58 9	59 8	62 4
12,360	44 5	42 2	45 3	40 6	46 1	38 2	43 7	45 5	37 7	42 4	44 9	36 0	42 4	32 3	33 7	37 3	43 3
16,410	10 0	96	10 5	10 0	11 2	97	11 6	11 7	10 6	11 6	11 7	10 6	11 8	10 5	99	11 0	14 4
20,460	36	35	37	36	39	35	41	41	39	40	40	38	40	38	35	39	54
24,280	9	10	10	10	12	11	12	12	12	12	13	12	13	13	12	14	17

28,325	3	3	3	3	4	3	4	4	4	4	5	4	4	4	4	5	5
32,370	1	1	1	1	2	1	2	2	2	2	2	2	2	2	2	2	2
36,420	0	0	0	1	1	1	1	1	1	1	1	1	1	1	1	1	1
40,015	0	0	0	0	0	0	0	0	0	0	0	0	0	0	0	0	0

Table 23: Load spectra distribution for tandem axles

Axle Load (Lbs)	Tandem Axles each 1000 vehicles																
	1	2	3	4	5	6	7	8	9	10	11	12	13	14	15	16	17
9,000	33 9	31 4	32 4	27 7	31 4	24 4	27 0	28 7	22 5	24 5	26 0	19 4	22 2	13 4	14 2	17 9	19 1
17,100	40 9	37 5	38 8	32 6	36 9	28 0	30 9	33 4	24 7	28 7	30 4	20 5	25 8	13 5	15 2	18 3	20 6
24,720	32 2	29 5	31 2	25 5	30 2	21 8	24 8	27 5	18 9	22 9	25 6	15 5	21 1	10 0	12 3	15 3	18 3
32,820	33 5	30 3	31 8	25 9	30 4	21 5	24 5	27 2	18 0	21 8	24 1	14 0	19 6	87	11 1	13 8	12 1
40,920	11 3	10 3	11 4	88	11 4	74	92	10 4	62	81	98	50	78	31	44	60	41
48,560	22	20	24	18	25	16	21	24	14	19	25	12	20	8	12	17	11
56,650	4	4	6	4	7	4	5	6	3	5	7	3	6	2	4	5	3
64,740	1	1	2	1	2	1	2	2	1	1	2	1	2	1	1	2	1
72,840	1	0	1	0	1	0	1	1	0	1	1	0	1	0	0	1	0
80,030	0	0	0	0	0	0	0	0	0	0	0	0	0	0	0	0	0

Table 24: Load spectra distribution for tridem axles

Axle Load (Lbs)	Tridem Axles each 1000 vehicles																
	1	2	3	4	5	6	7	8	9	10	11	12	13	14	15	16	17
13,500	5	6	20	7	24	8	25	28	5	17	41	11	39	6	22	23	3
25,650	3	3	10	4	13	4	13	15	3	9	22	6	20	4	12	13	2
37,080	3	3	11	5	15	5	14	17	4	10	25	7	22	6	14	16	2



**5.2- Typical values of Resilient Modulus and Poisson's ratio**

Type of Soil	Minimum Resilient Modulus (PSI)	Maximum Resilient Modulus (PSI)	Mean Resilient Modulus (PSI)	Poisson's Ratio
A-1	38,500	42,000	40,000	0.35
A-1-b	35,500	40,000	38,000	0.35
A-2-4	28,000	37,500	32,000	0.35
A-2-5	24,000	33,000	28,000	0.35
A-2-6	21,500	31,000	26,000	0.35
A-2-7	21,500	28,000	24,000	0.35
A-3	24,500	35,500	29,000	0.35
A-4	21,500	29,000	24,000	0.35
A-5	17,000	25,500	20,000	0.40
A-6	13,500	24,000	17,000	0.40
A-7-5	8,000	17,500	12,000	0.40
A-7-6	5,000	13,500	8,000	0.40
CH	5,000	13,500	8,000	0.40
MH	8,000	17,500	11,500	0.40
CL	13,500	24,000	17,000	0.40
ML	17,000	25,500	20,000	0.40
SW	28,000	37,500	32,000	0.40
SP	24,000	33,000	28,000	0.40
SW-SC	21,500	31,000	25,500	0.40
SW-SM	24,000	33,000	28,000	0.40

SP-SC	21,500	31,000	25,500	0.40
SP-SM	24,000	33,000	28,000	0.40
SC	21,500	28,000	24,000	0.40
SM	28,000	37,500	32,000	0.35
GW	39,500	42,000	41,000	0.35
GP	35,500	40,000	38,000	0.35
GW-GC	28,000	40,000	34,500	0.35
GW-GM	35,500	40,500	38,500	0.35
GP-GC	28,000	39,000	34,000	0.35
GP-GM	31,000	40,000	36,000	0.35
GC	24,000	37,500	31,000	0.35
GM	33,000	42,000	38,500	0.35
Concrete Pavement	1,450,000	4,200,000	4,650,000	0.15
Asphalt Pavement	72,500	26,000	14,500	0.35
CTB	435,000	870,000	725,000	0.15
ATB	43,500	116,000	72,500	0.35

## References

- AASHTO (1993). "Guide for Design of Pavement Structures." American Association of State Highway and Transportation Officials, Washington DC.
- ARA, Inc. (2007). Interim Mechanistic-Empirical Pavement Design Guide Manual of Practice. Final Draft. National Cooperative Highway Research Program Project 1-37A.
- BORDELON, A., ROESLER, J.R., AND HILLER, J.E., Mechanistic-Empirical Design Concepts for Jointed Plain Concrete Pavements in Illinois, Final Report, FHWA-ICT-09-052, Illinois Center for Transportation, University of Illinois, Urbana, IL, July 2009, 255 pp. Cervantes, V., and Roesler, J. (2009). "Performance of Concrete Pavements with Optimized Slab Geometry." Urbana Illinois.
- CONTROLES Y MEDICIONES SA, Reporte Evaluación de la calidad de la superficie del pavimento, Guatemala 2006
- COVARRUBIAS T. Juan Pablo, Andahur, Daniel. Análisis del Comportamiento de Pavimentos Delgados en Condiciones de Carga Pesada Modelación con Software de Elementos Finitos ISLAB 2000, Enero, 2006
- COVARRUBIAS V, JUAN PABLO, COVARRUBIAS, T and ROESLER, J.R. Design of concrete slabs with optimized geometry, Seville 2010
- Covarrubias, J. P. T., and Covarrubias, J. P. "'TC' Design for Thin Concrete Pavements." Proc., 9th International Conference on Concrete Pavements: The Golden Gate to Tomorrow's Concrete Pavements, 905-917.
- ERES CONSULTANTS, ISLAB 2000. Finite Element Program for the Analysis of Rigid Pavements, Version 1.1, USA, 1999. FHWA (2009). "Long Term Pavement Performance Database." Federal Highway Administration.
- Ioannides, A. M., and Khazanovich, L. (1998). "General Formulation for Multilayered Pavement Systems." Journal of Transportation Engineering, 124(1), 82-90.
- Ioannides, A. M., Khazanovich, L., and Becque, J. L. (1992). "Structural Evaluation of Base Layers in Concrete Pavement Systems." Transportation Research Record(1370), 20-28.
- Khazanovich, L. (1994). "Structural Analysis of Multi-Layered Concrete Pavement Systems." Ph.D., University of Illinois Urbana-Champaign, Urbana.
- Khazanovich, L., Darter, M. I., and Yu, H. T. (2004). "Mechanistic-Empirical Model to Predict Transverse Joint Faulting." Transportation Research Record(1896), 34-45.
- Khazanovich, L., Selezneva, O., Yu, H. T., and Darter, M. I. (2001). "Development of Rapid Solutions for Prediction of Critical Continuously Reinforced Concrete Pavement Stresses." Transportation Research Record(1778), 64-72.
- Khazanovich, L., Yu, H. T., Rao, S., Galasova, K., Shats, E., and Jones, R. 2000. ISLAB2000 - Finite Element Analysis Program for Rigid and Composite Pavements ERES Consultants, Champaign, Illinois.
- Korenev, B. G., and Chernigovskaya, E. I. (1962). "Analysis of Plates on Elastic Foundation." Gosstroizdat.
- LARRAIN, C. Análisis Teórico-Experimental del Comportamiento de Losas de Hormigón de Pavimentos, MSc Thesis, School of Engineering, Catholic University of Chile, 1985, 280 pp. Miner, M. (1945). "Cumulative Damage in Fatigue." Transactions of the ASME, 67, A159-A164.
- NCHRP. 2006. Mechanistic Empirical Pavement Design Guide, version 1.1 Transportation Research Board, Washington DC.
- Westergaard, H. M. (1927). "Theory of Concrete Pavement Design." Proceedings of the Highway Research Board.

